2

THE ORIGIN AND DIFFERENTIATION OF THE EARTH

The origin and differentiation of the Earth – the big picture

The Universe was already 9 billion years old when our solar system was born at 4.567 Ga. The compression and collapse of a gas cloud in the interstellar medium gave rise to a flattened disk of gas and dust rotating around an otherwise nondescript, medium-sized star. It was in this rotating disk of gas and dust – the primitive solar nebula – that our planetary system was formed.

The original building blocks of the Earth are thought to be preserved in a group of primitive meteorites known as the carbonaceous chondrites. These contain inclusions rich in calcium–aluminum minerals which formed at high temperature within 10^4–10^5 years of the formation of the solar system. Also present are chondrules, olivine-rich spheroidal melt droplets, a few millimeters in diameter, which formed within the first 4 Ma of Solar System history.

The formation of the Earth can be explained by the "standard model of planetary formation," in which dust fragments, including the types described above from meteorites, accumulate through the process of accretion – first, into kilometer-sized planetesimals over a timescale of 10^4 years, and then into planetary embryos – up to 4,000 km in diameter – over an interval of 10^6 years. The final stage of planetary accretion took place over 10^7–10^8 years and involved collisions between a relatively small number of large planetary bodies, giving rise to "giant impacts." These late, large-magnitude impacts are thought to have had a profound influence on the earliest history of the Earth System.

The latest of these involved an oblique collision between the proto-Earth and a body the size of Mars, at about 30 Ma after the formation of the solar system. This impact generated a huge amount of thermal energy so that a significant portion of the Earth was vaporized. This vapor coalesced around the Earth and cooled to form the Moon. A consequence of this impact is that a significant proportion of the Earth's mass would have been molten, creating what has become known as a magma ocean.

Similarly, the Earth's core is thought to have formed during the early stages of accretion, perhaps by as early as 10 Ma after the formation of the solar system. Geochemical constraints require the core to have also formed within a deep magma ocean, with liquid metal separating from a silicate melt at depths as great as 1,000 km.

Although the circumstantial evidence for the existence of a terrestrial magma ocean is strong, independent geochemical evidence has been hard to find. Recently however, the first geochemical clues of mineral fractionation with a deep molten mantle have been found, supporting the terrestrial magma ocean concept.

It was in this earliest Earth System that there was the strongest interaction between the different Earth reservoirs. There were intense, dynamic interactions between core, mantle, proto-ocean, and atmosphere. In addition there was probably an early basaltic crust, now long since lost by recycling into the mantle.

2.1 The origin and early history of the Universe

Enquiring into the origin of the Universe is to pose one of the most fundamental and difficult scientific questions of all. It also brings us into a very rapidly advancing and exciting field of science. In recent decades, cosmology has advanced extremely rapidly, and in the last few years has begun to provide the first self-consistent answers to age-old questions (Silk, 1994; Longair, 1998; Rees, 2000).

In many ways, the question of the origin of the Universe is far beyond the scope of this book. Nevertheless, in the context of understanding the origin of the Earth a brief review of the cosmological background is provided here. This is in fact necessary, for some of the fundamental features of the Earth system can only be understood within a framework of cosmology and cosmochemistry. There are two specific areas that are important within Earth System Science. The first is that the elemental abundances in the early solar system are a function of its setting within the galaxy and this "cosmic geography" ultimately determines the "raw materials" of the terrestrial planets. A second reason is that a planetary view of the Earth provides insight into the ultimate Earth system, in which there was profound, dynamic interaction between what are now the different components of the modern Earth system.

2.1.1 The Big Bang theory

The prevailing theory of the origin and evolution of the Universe is the Big Bang theory. According to this theory, about 14 billion years ago the Universe expanded to its present enormous volume from an initial volume, which was effectively zero. Three sets of observations have profoundly shaped the way in which we think about our Universe and led to the Big Bang theory. First was the discovery that our Universe is expanding. Second, there were predictions about the abundances of the light elements H, He, and Li in the Universe, and third was the discovery made by Penzias and Wilson (1965) that our part of the Universe is filled with microwave radiation.

2.1.2 Evidence for the Big Bang theory

2.1.2.1 An expanding Universe

Hubble (1929) discovered that there is a simple, linear relationship between the distance to a remote galaxy and the cosmological redshift – the redshift in the spectral lines from that galaxy (Hubble, 1929). Hubble's observations showed that the greater the distance to a galaxy, the greater the redshift in its spectral lines. These measurements strongly indicated that galaxies appear to be moving away from us with speeds proportional to their distance. The net effect of this motion is that, as time goes on, the galaxies are getting further and further apart. A very important consequence of these observations is that at some point in the past all matter must have been concentrated in one place. Astronomers define this point in time as the beginning of the Universe. At this time all the matter of the Universe was concentrated in an infinitely small volume with a state of infinite density.

2.1.2.2 The abundance of the light elements

The Big Bang theory predicts that the early universe was very hot. In the early stages of the formation of the Universe the light elements H (and its isotope deuterium), He, and Li were formed during the "Big Bang nucleosynthesis." The deuterium found today in the interstellar medium could only have formed at the beginning of the Universe (Songaila et al., 1994). Calculations based upon the initial ratio of protons and neutrons suggest that if the Big Bang theory is correct then about 24% of the ordinary matter in the Universe will be He and the rest hydrogen (Schramm & Turner, 1998). This value is in good agreement with recent observations indicating that the Big Bang theory passes one of its key "tests."

2.1.2.3 The Cosmic Microwave Background

If the early Universe was extremely hot, it is possible that, even today, the remnants of this initial fireball might be detected. Support for this hypothesis came from the discovery by Penzias and Wilson (1965) of what came to be known as the Cosmic Microwave Background. This discovery coincided with the work of theoretical physicists who showed that if the

Universe began with a hot Big Bang, then the Universe should be filled with electromagnetic radiation cooled from the early fireball to a temperature of around a few Kelvin. In subsequent years a large number of direct measurements of the Cosmic Microwave Background at different wavelengths yielded an intensity–wavelength plot which had the characteristics of black body radiation at 2.73 K. This is the remnant of the initial fireball of the Big Bang.

2.1.3 The current state of the Big Bang theory

The Big Bang theory allows us to pose (and answer) a number of fundamental questions about the Universe. These include questions about the nature of matter and energy in the Universe, about its speed of expansion and whether this is changing with time, about the age of the Universe, and about its ultimate fate – whether or not it will continue to expand. Cosmologists have debated these issues for decades, but some recent exciting results have begun to provide some significant answers.

Central in this discussion was the balance between an expanding Universe from the initial impulse of the Big Bang and the counteracting influence of the gravitational attraction of matter in the Universe. In the 1990s astronomers found a way of measuring the expansion rate of the Universe at different times in its history and found, to their great surprise, that the Universe is expanding faster now than it did earlier in its history (Reiss et al., 2001). This observation led to the recognition of what has become known as "dark energy," a force that appears to counteract the effects of gravity (Bahcall et al., 1999). Understanding the nature and origin of dark energy is one of the outstanding problems of modern cosmology.

More recently, in 2002 the Wilkinson microwave anisotropy probe (WMAP) was launched to map the fine detail of the Cosmic Microwave Background. After a year of mapping the first results were published in 2003 (Bennett et al., 2003), with some far-reaching conclusions. A best-fit cosmological model for the Cosmic Microwave Background is satisfied by a Universe composed of only 4.4% of ordinary baryonic matter (protons and neutrons). The rest is made up of nonbaryonic matter, identified as dark matter (22% of the Universe), that is, particles, which can only be detected by their gravitational effect, and dark energy, making up 73% of the Universe (Fig. 2.1). They found that their estimate of the total mass–energy of the Universe was in good agreement with earlier results from high altitude balloon experiments (e.g. de Bernadis et al., 2000) signifying that the geometry of the Universe is flat. These data strongly support the theory of the inflation of the Universe – that is, an extremely rapid expansion of the Universe shortly after the Big Bang.

In its present form, standard Big-Bang cosmology is a very open subject, for it contains three important elements – dark matter, dark energy, and inflation – about which there is

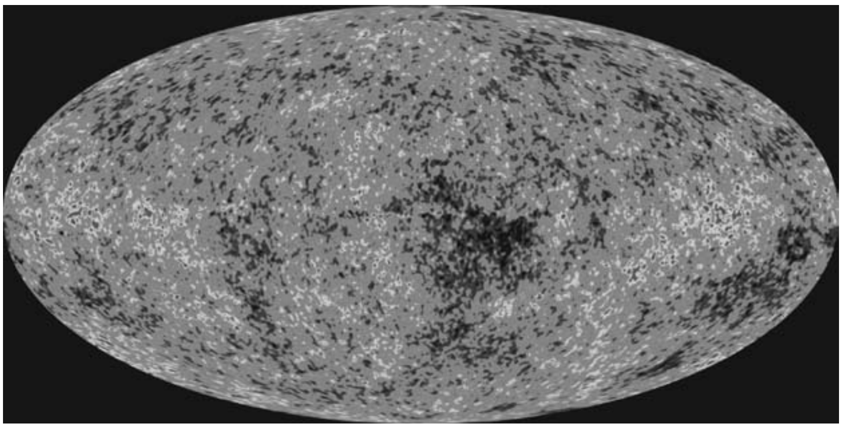

FIGURE 2.1 A WMAP image of the infant universe showing 14 billion year old temperature fluctuations (shown as differences in grey shading) that correspond to the seeds of galaxies (from http://map.gsfc.nasa.gov/m_or.html, courtesy of NASA/WMAP Science team).

no known mechanism, and therefore may be subject to significant shifts in understanding in the future.

The best-fit cosmological model for the Cosmic Microwave Background from the WMAP also precisely constrains the age of the Universe. This is a welcome contribution to what has been a comparatively inexact science, with two irreconcilable camps preferring either a "young" 10 Ga or "old" 20 Ga age for the Universe. A number of different approaches had been used such as the calculation of velocity–distance relationships measured from galaxies, the application of radioactive dating methods to old stars (Cayrel et al., 2001), and relationships between the luminosity and mass of a star. The recent WMAP result indicates that the age of the Universe is a precise 13.7 ± 0.2 Ga (Bennett et al., 2003). This is in good agreement with an earlier less precise result of 13.4 ± 1.6 Ga based on the rate of expansion of the Universe (Lineweaver, 1999). However, all results in this field are model-dependent and may be the subject of change in the future.

2.1.4 The early history of the Universe

Current thinking in cosmology indicates that the history of the Universe may be described in the following stages (Fig. 2.2):

An initial singularity. At the beginning of the Universe, 13.7 billion years ago, all matter was in one place at a single instant; this event in cosmological parlance is known as a "singularity." This term describes the inference that an infinitely large amount of matter is gathered at a single point in space-time.

The Big Bang. At the Big Bang there was a huge expansion of matter, an expansion that has continued ever since.

Inflation. Between 10^{-50} and 10^{-30} s after the Big Bang there was a particularly rapid expansion of the Universe. This process is known as the inflation of the Universe and represents the first burst of growth of the Universe. During inflation the part of the Universe that we see today expanded by a factor of 10^{60}. When the Universe was only one second old temperatures were of the order of 10 billion degrees. At that point the universe was permeated with radiation and subatomic particles. When the Universe was a few minutes old and temperatures were about 1 million degrees protons and neutrons formed atomic nuclei leading to the production of primordial hydrogen and helium ions.

An opaque Universe After 100,000 yr conditions in the Universe were similar to those inside

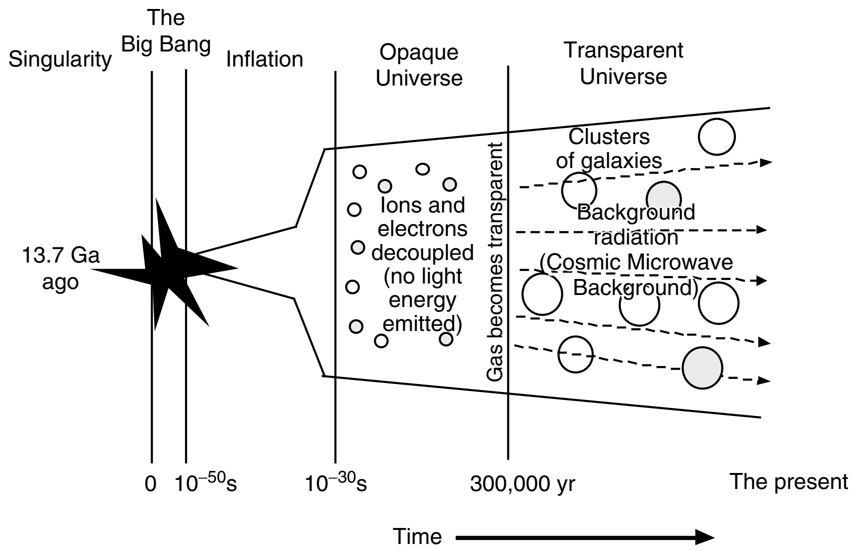

FIGURE 2.2 The origin, inflation, and expansion of the Universe from the initial singularity to the present.

the sun today. An almost uniform plasma of electrons, hydrogen, and helium ions filled the Universe. At this time the free electrons acted as a block to photons – generated from the light energy generated in the Big Bang, and prevented them escaping, rendering the early Universe opaque.

A transparent Universe. After 300,000 yr temperatures dropped to 4,500 K and gave rise to the formation of atomic matter, and atoms of hydrogen, helium, and deuterium were formed. Because electrons were removed from the plasma through the formation of atoms, radiation streamed out and the Universe became transparent. Initially the Universe contained abundant ultraviolet- and X-rays, now cooled down to microwave wavelengths. This is what is recorded as the Cosmic Background radiation.

The present Universe. As the universe continues to expand the initial radiation will appear to be derived from a much cooler body. Hence today the Cosmic Background radiation is 2.73 degrees above absolute zero.

It is a long journey from the formation of the Universe at 13.7 Ga ago to the formation of the Earth at about 4.57 Ga. This journey is the subject of the next sections of this chapter, and in them we shall consider the relationship between the Earth and its host – the solar system. In so doing we shall discuss the processes which have led to star formation, to the formation of the chemical elements, the condensation of the solar system, and ultimately to a model for planetary accretion and hence the Earth.

2.2 Star Formation

In this section we consider the processes which led from the Big Bang to the formation of stars and galaxies.

2.2.1 The anisotropy of the Universe

As cosmologists began to accumulate measurements of the Cosmic Background radiation at the edge of the Universe they were impressed by the uniformity of the results. However, many theorists predicted that in detail the results should not be uniform, leading to a search for microscale variability in the cosmic background radiation. This was first discovered using a differential microwave radiometer on the COBE space probe and demonstrated that the Cosmic Microwave background was very slightly variable on the scale of one part in 100,000. A better resolution of this temperature fluctuation was obtained by the WMAP (Bennett et al., 2003). These results are shown in Fig. 2.1 and provide a detailed map of the temperature fluctuations in the Universe at the beginning of time, demonstrating that matter and energy were not evenly distributed in the very early Universe.

This unevenness in the distribution of matter and energy has been described as the "lumpiness," or more correctly, the anisotropy of the early Universe. Elsewhere it is stated that the Universe is homogeneous or isotropic. This is not a contradiction, rather a difference of scale. On a large scale the Universe is homogeneous and everywhere has a temperature of 2.73 K at its edge. On a fine scale however, microvariations in temperature have been measured.

The significance of this variation in the intensity of the Cosmic Microwave Background is that it shows how matter and energy were distributed when the Universe was still very young. It is thought that these early inhomogeneities subsequently developed into the regions in the present Universe where there is matter, that is, galaxies and galaxy clusters, and those regions from which matter is, absent – space. The early inhomogeneous distribution of matter also reflects an inhomogeneous distribution of density, and it is these initial density differences that gave rise to small differences in gravitational forces which began to draw matter together.

2.2.2 The formation of galaxies

Primordial gas clouds, composed of hydrogen and helium, are thought to be the beginnings of galaxies and represent the first large-scale structures to form in the evolving Universe. These huge gas clouds with masses 10^{15}–10^{16} greater than that of the sun (that is, 10^4–10^5 times greater than our own galaxy, the Milky

Way), formed due to gravitational forces working against the expansion of the Universe.

Just as primordial gas clouds formed through weak, small scale density fluctuations in the Universe, so also a similar process led to their fragmentation into molecular gas clouds, with dimensions greater than 10^{14} km, and masses a million times greater than the sun. This process took place in the first few hundred million years of the Universe when it was more compact than at the present time. It was a chaotic, turbulent process, in which strong gravitational forces hurled matter together at supersonic speeds. Fragments of the gas cloud, compressed by the effects of density and by shock waves, collided into each other forming the basis of what we now recognize as galaxies.

2.2.3 Galaxies

Today galaxies are huge concentrations of stars, that range in size from 80,000 to 150,000 light years in diameter. (A light year is the distance traveled at the speed of light in a year). Within this huge volume, galaxies contain very large numbers of individual stars – ca. 100 billion. There are at least 10 billion galaxies in the Universe.

There are two main groups of galaxies, spiral galaxies and elliptical galaxies. Spiral galaxies (see Fig. 2.3) are disk-shaped, contain abundant dust and gas and are home to regions of active star formation. Elliptical galaxies are spheroidal in shape, contain very little dust and gas, are not host to regions of star formation and so contain mainly old stars. Our own galaxy, the Milky Way, is of the spiral type. The spiral arms are thought to have been produced by density waves which sweep through the galaxy. The Sun is located in the outskirts of the Milky Way galaxy, between two spiral arms. It is these arms that form the Milky Way appearance at night.

In addition to the two main groups of galaxies, there are a number of other galaxy types. Of these Quasars (quasi-stellar objects) are galaxies with very energetic nuclei. They form small, very bright objects which emit as much as a 100 times the radiation of a normal galaxy. They only exist at immense distances and are thought to represent an early stage of

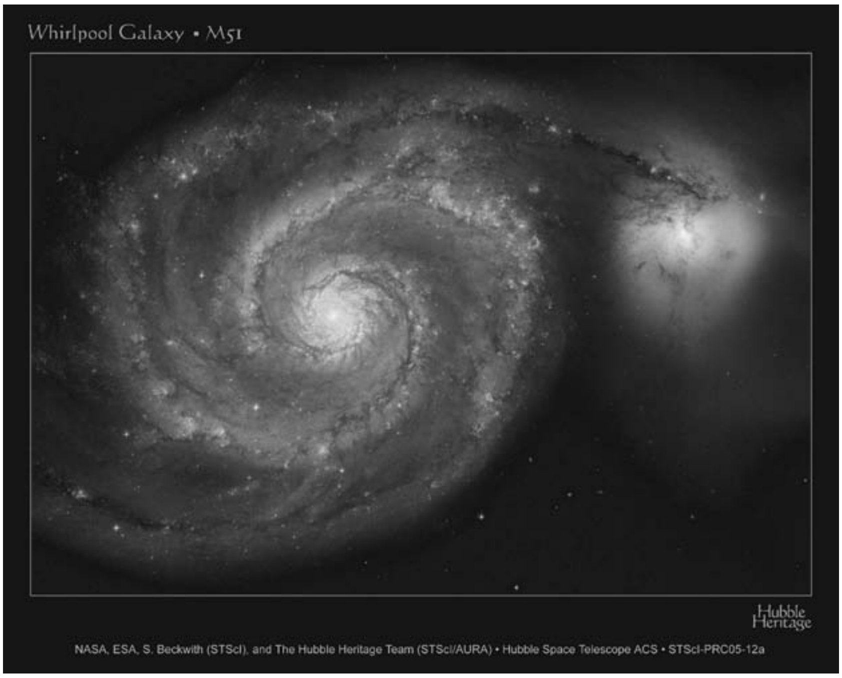

FIGURE 2.3 A typical spiral galaxy – the Whirlpool Galaxy, M51 and companion galaxy (from the HubbleSite picture gallery http://hubblesite.org/, Credit NASA, http://www.nasa.gov/, ESA, http://www.spacetelescope.org/, S. Beckwith (STSci), http://www.stsci.edu/, and the Hubble Heritage team (STSci/AURA), http://heritage.stsci.edu (http://www.stsci. edu/and http://www.aura-astronomy.org/)).

formation of large galaxies, formed, in part, through galactic collisions which took place early in the history of the Universe.

2.2.4 The process of star formation

As large molecular clouds fragment and collapse, star formation can take place. This process is triggered by density inhomogeneities in the gas cloud, producing regions which become gravitationally unstable and contract. Some stars appear to have formed in groups and are geometrically arranged, implying that a particular "event" might have initiated their genesis. Such an event could be caused by shock waves propagated from supernovae explosions or by density waves within the arms of a spiral galaxy. The process of gravitational collapse within a star leads to an increase in the temperature and pressure of the gas at its center, igniting thermonuclear fusion and turning hydrogen into helium. The radiation from this process leads to an outward pressure preventing further collapse.

The key features of stars which are of interest to astronomers are their mass, their luminosity, their surface temperature, and their distance from us. These parameters are used to classify stars and place them into an evolutionary sequence. A widely used classification diagram, based on optical data for stars, is the Hertzsprung–Russell Diagram (the H–R diagram) which is a plot of stellar luminosity versus effective surface temperature. The luminosity of a star is a function of its radius and effective temperature. The surface temperature is determined from its color and is vastly different from temperatures in the core of the star. For example, our sun has a surface temperature of about 5,700 K but a core temperature of 14 million K.

Data from nearby stars measured by the Hipparcos satellite and displayed on a Hertzsprung–Russell Diagram show four main groups of stars (Fig. 2.4). These are the following:

Main sequence stars, which make up 90% of all stars, define a curved trend across the center of the diagram, showing a relationship between mass and luminosity, such that large stars have a high luminosity and a high surface temperature and small stars have a lower luminosity and surface temperature. Hot, large stars burn up quickly and have a short life span whereas smaller cooler stars are more long-lived. For example a star in the top left of the diagram will last for about 10 million years before going supernova, whereas a star similar to our Sun will probably last 10 billion years.

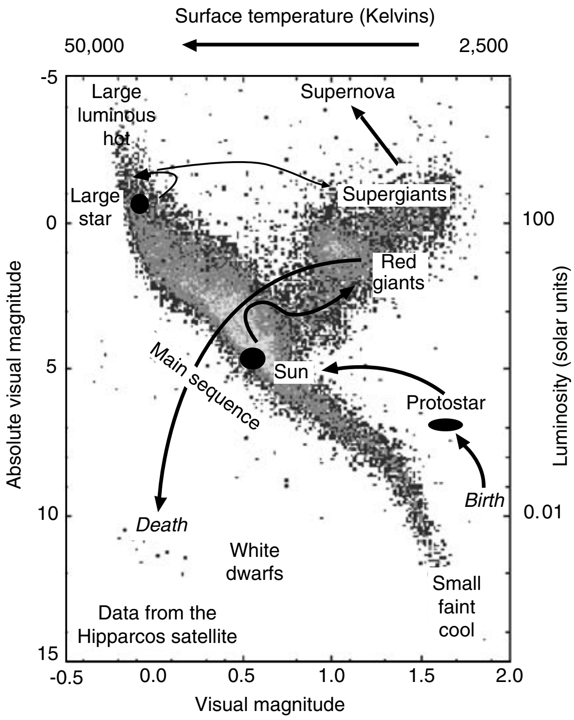

FIGURE 2.4 Hertzsprung–Russel diagram for the classification of stars. The data in this diagram are taken from the Hipparcos satellite which measured the properties of more than 10,000 nearby stars. Key variables are the relationship between the luminosity of the star (relative to the sun) or absolute visual magnitude, and its color index – the inverse of the surface temperature. The data in this diagram show the relative importance of the different types of star. The arrows show a typical birth to death cycle of a small star (lower part of diagram) and of a large star with a mass 25 times that of the sun (upper part of diagram).

Red giants are stars which are cooler, but more luminous than stars on the main trend. These are stars which have exhausted their supply of hydrogen and are now burning helium. This process causes them to expand. *Super giants* are similarly stars which are more luminous but much cooler than main sequence stars.

White Dwarfs are stars which are less luminous than main trend stars. These stars have exhausted H and He in their core and can be thought of as dead stars radiating away their energy.

2.2.5 The evolutionary cycle of stars

The cycle of birth–life–death for a star may be charted on a Hertzsprung–Russell diagram as illustrated in Fig. 2.4. Most stars evolve onto the main sequence and then into the Dwarf stage as follows (Lewis, 2004):

- An interstellar cloud of hydrogen and helium gas and dust is compressed. The contraction leads to an increase in density and a lowering of transparency and temperature, and simple molecules form.
- Continued contraction, now driven by gravitational collapse causes temperatures to rise. Molecules break down to atoms, ions, and subatomic particles. The highest temperatures are in the center of the mass, and it is here that nuclear burning begins giving birth to a protostar (Fig. 2.4).
- The newly-formed star subsequently evolves to be part of the main sequence of stars. The precise position on the main sequence depends upon the mass of hydrogen present in the star. At this point in its life temperatures in the core of the star are as high as 10^7K. Nuclear fusion takes place within the center of the star and helium is formed. At higher temperatures, above 10^8K, He reacts through nuclear fusion to form heavier elements such as carbon and oxygen (see Section 2.2.6.1). It is at this stage of stellar evolution that planetary formation may take place, although these processes are entirely unrelated to the high pressures and temperatures that ignite the fusion.
- Evidence from open star clusters shows that with aging stars migrate to the right on a H–R diagram and eventually convert into a Red Giant (Fig. 2.4). At this stage two separate thermonuclear processes are taking place in both the core and the shell. Hydrogen burning in the shell leads to massive expansion of up to 100 times the diameter of the original star.
- The final stage of stellar evolution depends upon star mass. A star smaller than the sun is unable to burn He and so ends up as the core of a Red Giant, which quickly lose its outer layers to space and fades away as a White Dwarf (Fig. 2.4). In larger stars, as the core collapses, temperatures and pressures become high enough for He to ignite and be converted to C and O in a supernova, and there is a huge explosion marking the end of their life (Fig. 2.4). Within the dense supernovae, neutron stars may form as the extremely dense endpoint in the life of a star.

2.2.6 The origin of the elements

Stars shine because nuclear reactions take place in their core. When these reactions take place there is a slight lowering of the mass of the nuclei undergoing fusion which is liberated as energy. It is the fusion process which gives rise to the formation of the chemical elements.

2.2.6.1 The processes of element formation

Our understanding of the process of element formation is based upon the elemental composition of stars, deduced from optical spectra, and from the theoretical calculations and experimental observations of nuclear physics. From these different lines of reasoning it has become clear that nucleosynthesis took place in a variety of different environments. Although the principal processes of nucleosynthesis take place in stars and supernovae, it is now also recognized that the nucleosynthesis of some light elements happened during the Big Bang, and to a lesser extent through the interactions between cosmic rays and matter in interstellar space.

Cosmological nucleosynthesis. The elements H, and its isotope D, He, and Li were created in the first few moments of the Big Bang. These are the essential ingredients of the cosmos and the starting composition for all other elements. The ratio of He/H, in terms of the number of atoms, is about 25% as a consequence of this event, and although some additional He has been created in stellar nucleosynthesis (see below) the ratio in the Universe as a whole has remained essentially unchanged since the beginning of time.

Stellar nucleosynthesis. Elements with atomic masses up to that of iron (^{56}Fe) are created in stars through a variety of different reactions, taking place over a wide range of temperatures.

Hydrogen burning and helium production. Hydrogen burns in the core of a star to form ^{4}He through either the proton–proton chain reaction, which takes place at 5×10^{6} K or at higher temperatures ($> 20 \times 10^{6}$ K) through the carbon cycle (the C–N–O cycle) in which carbon acts as a nuclear catalyst in the production of He. This process is also known as the quiescent burning phase of a star and is a slow process which takes billions of years and covers much of the life of a star. Our sun is currently in this phase.

Helium burning to form carbon and oxygen. As the hydrogen in a star is used up, the star contracts and its temperature rises to greater than 10^{8} K. At this stage nuclear reactions take place which permit the synthesis of the elements carbon, nitrogen, and oxygen, from helium. ^{12}C forms from ^{4}He, through what is known as the triple alpha reaction, and when sufficient ^{12}C is present, further reaction leads to the formation of ^{16}O.

Carbon and oxygen burning. When the helium is almost completely consumed then the carbon and oxygen can be transformed into elements with masses up to that of silicon. This takes place after the stellar core has contracted further and increased in temperature. In detail carbon fusion reactions (^{12}C) lead to the formation of ^{24}Mg, ^{23}Na, and ^{20}Ne at about 6×10^{8} K. Oxygen fusion reactions lead to the formation of ^{32}S, ^{31}P, ^{31}S, and ^{28}Si at about 10^{9} K.

Silicon burning. As carbon and oxygen burning proceeds the stellar core becomes enriched in Si and is at temperatures of about 10^{9} K. At these temperatures nuclear reactions in the stellar core induced by photons lead to the formation of elements with masses up to that of iron. Elements heavier than Si cannot be formed by the process of nuclear fusion because beyond this point the nuclear reactions cease to be an energy source. The most energetic fusion reaction is hydrogen burning; a lesser amount of energy is produced by He-burning, even less from C and O, and progressively less until Fe is reached at which point no energy is released at all.

Explosive burning in a supernova. In contrast to the nuclear reactions thus far described, the formation of elements beyond the mass 56 (Fe) consumes energy. This process is that of neutron capture and involves the absorption of neutrons by the atomic nucleus. Hence heavier elements such as silver, gold, or lead can only be formed in a highly energetic environment within a star, such as found in a supernova explosion, because only in this environment is sufficient energy released to allow the energy-inefficient process of heavy-element formation to take place. Supernovae explosions are the endpoint of large stars and represent the violent collapse of a Fe-rich stellar core, during which neutrons, produced in the core collapse, are captured by other nuclei. They are built into heavy nuclei, through rapid neutron capture, up to the elements Th and U. Hence, the reason that the heavy elements are so rare is because the process by which they are formed is rare – approximately only one in a million stars is massive enough to go supernovae.

2.2.6.2 The interpretation of solar elemental abundances

Solar element abundances (Anders & Grevesse, 1989) are plotted against increasing atomic numbers in Fig. 2.5. These data were obtained by the optical analysis of the solar spectrum. Abundances are measured relative to 1 million silicon atoms on a logarithmic scale.

There are three important observations to be made from this graph (Fig. 2.5):

First, the graph has an overall smooth trend from light to heavy elements, indicating that solar abundances are greatest for light elements and least for heavy elements. This is consistent with the discussion above, in which H and He abundances date from the Big Bang, and are the starting material from which all other elements have been built. It is also consistent with the burning of He to form C and O, and the burning of C and O to form successively heavier elements.

Second, superimposed upon the smooth trend is a smaller scale irregularity, such that

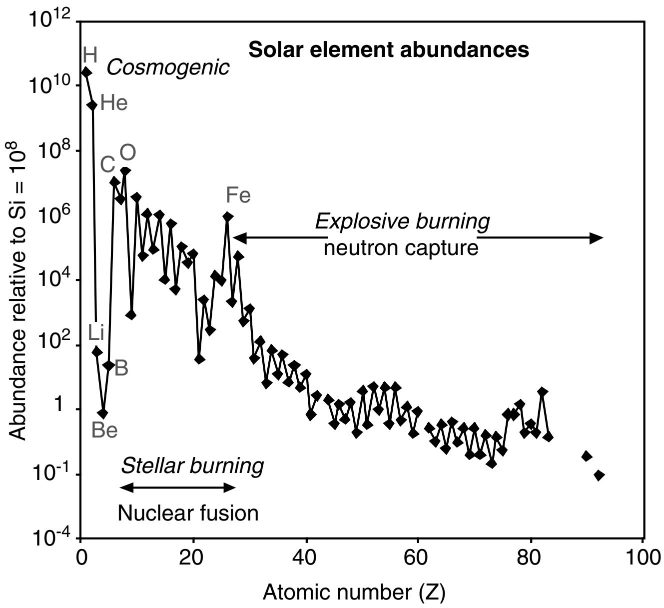

FIGURE 2.5 Abundances of elements in the sun, by atomic number, relative to solar Si = 10^6 (Data from Anders & Grevesse, 1989).

elements with even atomic numbers have higher abundances than those with odd atomic numbers. This can be explained by the greater stability of atomic nuclei with paired neutrons. Thus elements with even atomic numbers have the greater nuclear stability and therefore the greater abundance.

Third, some elements have anomalous abundances. Hydrogen and helium and iron have anomalously high concentrations. H and He have been discussed already. In the case of Fe this relates to the high binding energy and associated stability for Fe. The elements lithium, boron, and beryllium have anomalously low concentrations for they are not produced in stellar nucleosynthesis, as already discussed.

2.3 The condensation of the Solar System

The generally accepted model for the origin of the Solar System is that the Sun formed in a similar manner to any other medium angular momentum star, by the collapse of a region of gas in the interstellar medium. Compression associated with this collapse gives rise to an increase in temperature within the nebula and a small part (2–10%) of the gas condenses and forms a flattened disk of dust surrounding the star. This rotating disc of gas and dust is known as the primitive solar nebula, and it is from this that the planets and other bodies of the solar system formed. In this section we shall consider the processes which led to the formation of planets from the solar nebula, concentrating in particular on the formation of the Earth.

Our knowledge of the state of the primitive solar nebula in its early stages of development comes from a number of sources. These include the observations and calculations made by astronomers, from the principles of elemental behavior in planetary systems and from the study of meteorites and other extraterrestrial materials.

2.3.1 Evidence from astronomical observations

Astronomical observations of molecular clouds and young stellar objects provide the basis for our understanding of the early solar system (Cameron, 1995; Alexander et al., 2001). The first stage in this process is when a fragment of an interstellar molecular cloud collapses to form a disk-like nebula, or protoplanetary disk. This process normally takes between 10^6 and 10^7 years, although if triggered by interstellar shock waves it may be as short as 10^5 years.

During gravitational collapse within the molecular cloud, the adiabatic compression of gas from the interstellar fragment leads to the formation of an extremely hot core of gas, the central protostar. Most commonly, this central star becomes surrounded by a disk of condensed matter, which will become the planetary system. Once such a disk is formed all matter subsequently accreting to the star is processed through this disk. As the gravitational collapse of the molecular cloud continues adiabatic compression leads to the heating of the cloud, and the highest temperatures in the solar nebula are reached during this early stage of its development.

2.3.1.1 Solar nebula evolution

Astronomers recognize four classes (0 to III) of young stellar objects which can be used to track the development of the early solar system history. These are as follows. Class 0 objects are deeply embedded in their parental molecular cloud with most of their circumstellar mass still in the cloud rather than in the disk. A particular feature of this stage of solar nebula evolution is the presence of narrow bipolar jets of high velocity gas, which are ejected outward from center of the disc, perpendicular to the midplane. Excellent Hubble space telescope images of these jets have been observed on the young star HH30 (Boss, 1998). These jets continue into the later stages of nebular evolution and are a source of thermal energy in the otherwise cooling nebula. This stage of solar nebula evolution lasts about 10^4 years.

Class I objects are characterized by the build up of material in the disk followed by a burst of accretion onto the star. It is during this phase that the protostar acquires its main mass and grows rapidly over a timescale of 10^3–10^5 yr.

Class II objects are T Tauri stars, young stars with a cool surface but high luminosity, which lie above the Main Sequence trend on a H–R diagram, and are identified as protostars on Fig. 2.4. These stars retain well-developed dusty discs which typically have a mass of 0.02 solar masses. This stage may last from 10^5 to several million years. During this stage of solar nebula development, solar winds directed radially outward inhibit further accretion to the sun, and planetesimals and planets begin to form (Alexander et al., 2001). At this stage the nebula has lost most of its original (adiabatic) heat, facilitated by its disk-shape, and the condensation of water to ice is at the orbit of Jupiter.

Class III objects are weak line T Tauri stars (T Tauri stars in which the characteristic emission lines are only weakly observed in their optical spectra) and have little or no evidence of a disk. At this stage of solar nebula evolution, which may last between 3 and 30 Ma, the sun has formed, and the material of the nebula is being dissipated by solar winds in the inner part. In the outer part of the nebula material is dissipated by photo-evaporation caused by UV radiation from the solar wind. A positive pressure gradient near the inner edge of the nebula facilitates planetesimal formation.

Temperatures within the nebula vary over time and within the midplane of the disc decrease with distance from the core as shown in Fig. 2.6. They are also strongly dependent on the mass of the nebula, expressed as a fraction of the solar mass. The model in Fig. 2.6 is calculated for nebula masses of 0.02 and 0.04 solar masses (Boss, 1998).

A much cited example of a solar nebula is the main sequence star Beta Pictoris, which shows a central core, with a disc of matter rotating around the core (Fig. 2.7). Beta Pictoris is thought to be a young star (10–20 Ma old) showing the early stages of planetary formation and is "a somewhat messy planetary system caught in formation" (Artymowicz, 1997). It has a large ($>$1,000 AU) dust-dominated, thin disk surrounding the central star. The dust is of a similar composition to that of the solar system and contains Mg olivines and pyroxenes. There is no evidence of ice. Scattered light, from within the disk, analyzed using infrared thermal imaging has identified particles of all sizes – from the micron and millimeter scale. This distribution of dust particles has been used to infer the presence of

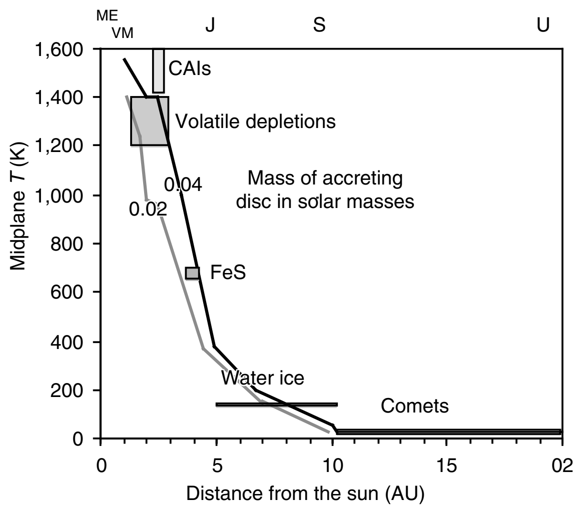

FIGURE 2.6 Midplane solar nebular temperatures (K) calculated for 0.04 and 0.02 solar masses in the accreting disk, and estimated temperatures from meteorites and comets, plotted against distance from the sun, expressed both as astronomical units (1 AU = Earth–Sun distance) (bottom) and planetary distance (top). The temperatures presented here are indicative only, as they are dependent upon the size of the disc and the thermal model used (after Boss, 1998).

planetesimal belts around the star (Okamoto et al., 2004; Telesco et al. 2005).

2.3.2 Evidence from cosmochemistry

A rather different approach to understanding the condensation of the solar nebula came from the work of the geochemist V.M. Goldschmidt carried out in the 1920s. Goldschmidt proposed, what has now become, a widely used geochemical classification of the elements. This work was in part based upon the study of meteorites, and so his classification is very relevant to the understanding of planetary processes.

Chemical elements display different chemical affinities, explained largely by their differing electronegativities, and may be classified into *lithophile elements* – those with an affinity for silicates and oxygen, c*halcophile elements* – those with an affinity for sulfur, *siderophile elements* – those with an affinity for metallic iron, and *atmophile elements* – those with an affinity for the gaseous atmosphere. Initially Goldschmidt's classification of the elements was helpful in understanding two rather different subjects – the differences

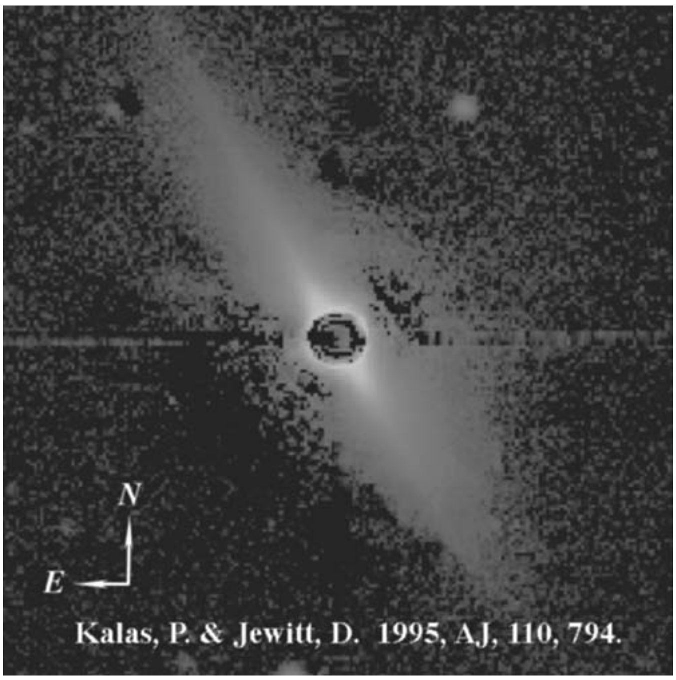

FIGURE 2.7 Beta Pictoris imaged in 1993, using the 2.2 m telescope of the Hawaii University at Mauna Kea. Kalas and Jewitt (1995) demonstrated that the disk is asymmetric, a feature that is often the result of gravitational perturbations from planets, although not thought to be the case in this study.

TEXT BOX 2.1 A geochemical classification of the elements

Geochemists have their own particular way of classifying the chemical elements as found in rocks and minerals.

Major elements are those chemical elements which make up the principal part of rocks. These are the elements which make up the main rock-forming minerals. They are normally reported as metals, but, since oxygen is also an important part of the Earth, by convention they are presented as percentages by weight of the metal oxide. They tend to be listed in the order – SiO_2, TiO_2, Al_2O_3, FeO, MnO, MgO, CaO, Na_2O, K_2O, and P_2O_5. Sometimes structurally bound water (listed as H_2O) may also make up several percentages by weight of the rock. Major element analyses should sum to about 100 wt%. A typical set of major element analyses is given in Chapter 3, Table 3.1.

Trace elements are those elements which do not normally make up rock-forming minerals in their own right, and are present at the part per million level (ppm) or lower. Over the past 50 years methods of determining the concentrations of trace elements in rocks have improved dramatically, so that determinations with precision at the parts per billion (ppb, 10^{-9}) level are not uncommon. A typical set of trace element analyses is given in Chapter 3, Table 3.2.

Minor elements are those elements which have concentrations between 1.0 and 0.1 wt%. They include elements such as Ti, Mn, K, and P. These elements may behave either as a major element or a trace element. For example, K may be present as several wt% in granite and may be part of a major rock-forming mineral (K-feldspar). In a basalt however, K may be present only at the ppm level, substituting for Na in plagioclase feldspar.

A geochemical classification of trace elements according to their position in the periodic table

It is useful in geochemistry to recognize particular groups of elements on the basis of their position in the periodic table. This is because their chemical similarities lead us to expect some similarity in their geochemical behavior in natural systems. In this text, reference will be made to:

- the *noble gases* (rare gases or inert gases) Ne, Ar, Kr, and Xe;
- the lanthanide series, or the *rare Earth elements (REE)*, as they are more normally known – elements 57 to 71 – La, Ce, Pr, Nd, (Pm), Sm, Eu, Gd, Tb, Dy, Ho, Er, Tm, Yb, and Lu;
- the *platinum group elements (PGE)*, Ru, Rh, Pd (elements 44–46), Os, Ir, and Pt (elements 76–78) and sometimes including Au (79);
- the *transition metals*, that is, the first transition series, Sc to Zn, elements 21 to 30.

A geochemical classification of trace elements according to their behavior during partial melting

During partial melting trace element behavior is governed by the preference of a particular element for its host (a mineral phase) or the melt phase. Elements which tend to become part of the melt are known as *incompatible elements*, and those which prefer to remain in the mineral phase are known as *compatible elements*. In detail this is governed by relationships between the particular element and the structure of the relevant mineral phase. The degree of incompatibility of a specific element in a particular mineral phase is expressed as the mineral–melt partition coefficient. Incompatible elements have mineral–melt partition coefficients < 1.0 and highly incompatible elements have partition coefficients $\ll 1.0$, whereas compatible elements have partition coefficients of > 1.0.

A geochemical classification of trace elements according to their ionic charge and size ratio

Small, highly charged ions behave differently from large ions with a low charge during geochemical processes. Small highly charged ions include metals such as Ti, Hf, Nb, and Zr and are known as the *high field strength elements (HFSE)*. These are elements which tend to be immobile when hydrous fluids react with a rock. Examples of larger ions carrying a low charge are Ba, Sr, and K. These are known as the large ion lithophile elements (LILE) or *low field strength elements*. These elements tend to be mobile in hydrous fluids.

A geochemical classification of the elements based upon their electronegativities

Lithophile elements are those which have a preference for a silicate host, whereas chalcophile elements have an affinity for sulfur and so will most frequently be found in sulfides. Siderophile elements are those which will partition preferentially into a metallic iron phase and so are enriched in the Earth's core and in iron meteorites. Atmophile elements prefer the gaseous phases of the Earth atmosphere. This classification is discussed more fully in Chapter 2, Section 2.3.2.

A cosmochemical classification of the elements based upon the solar condensation sequence

During the condensation of a solar nebula different mineral phases condense as the nebular temperature decreases. It is an understanding of this process which has led to an appreciation of the mineralogy of meteorites. Phases which condense at high temperatures (1850–1400 K) are known as *refractory*, whereas phases which cool at lower temperatures are know as *volatile*. Highly volatile phases condense below 640 K (see Section 2.3.2.1).

between the major meteorite groups (Section 2.3.3.1) and the differentiation of the Earth.

However, Goldschmidt's scheme only relates to the condensation of major elements into mineral phases. As the solar nebula hypothesis gained credence, it became clear that there are other element groupings which relate to the condensation of a high-temperature solar gas. These are: the *refractory elements* – those which formed above the condensation temperature of the Mg silicates and Fe–Ni metal, at 1,300–1,400 K, the *moderately volatile elements* – those formed in the range 1,300–670 K, and the *volatile elements* – those that formed below the condensation temperature of FeS, at 670 K (Larimer, 1988). Palme and O'Neill (2003) have proposed a cosmochemical/geochemical classification of the elements based on these two elemental groupings (Table 2.1).

2.3.2.1 The solar condensation sequence

The processes of vaporization and condensation are of major importance in the solar nebula. In order to systematize this process, Grossman (1972) used thermodynamic equilibria to calculate the composition of phases in equilibrium with a gas with cosmic element concentrations, at a pressure of 10^{-3} atm, and as a function of temperature. This work has subsequently been developed by others and is systematized in Lewis (2004). It is worth noting that in detail it is likely that the assumption of equilibrium conditions will not always apply to the condensation sequence (Wood, 1988). Nevertheless, observations of this type are invaluable in providing a first pass at interpreting the processes of planetary formation.

The solar condensation sequence may be described as a series of steps which describe the formation of phases, and subsequent reactions between phases, during the condensation of the solar gas (Lewis, 2004). These steps explain the main sequence of mineral phases forming in a solar nebula in relation to temperature and distance from the sun (Fig. 2.6). The temperatures indicated are taken from the adiabatic curve of Lewis (2004):

1 Formation of the refractory siderophiles. (The metals W, Os, Ir, and Re – although in reality concentrations are so low that these phases do not nucleate.)
2 Formation of refractory oxides (ca. 1,700 K). (Al, Ca, and Ti oxides such as corundum, spinel, perovskite, and some silicates. The phases also include the REEs and U and Th.)
3 Formation of iron–nickel metal (ca. 1450 K) (also included are the minor elements Co, Cu, Au, Pt, Ag and may include the nonmetals P, N, C).
4 Formation of magnesium silicates (ca. 1,420 K) (the principal components are olivine and Mg–pyroxene).
5 Formation of alkali metal silicates (ca. 1,020 K) (the major component is plagioclase feldspar).

TABLE 2.1 A cosmochemical and geochemical classification of the elements based upon their Lithophile/siderophile/chalcophile affinities and their refractory or volatile character (after Palme and O'Neill, 2003).

	Lithophile (silicate)	**Siderophile and chalcophile (metal and sulfide)**
Refractory *(T_c 1,850–1,400 K)*	Al, Ca, Ti, Be, Ba, Sc, V, Sr, Y, Zr, Nb, Ba, REE, Hf, Ta, Th, U, Pu	Mo, Ru, W, Re, Os, Ir, Pt
Main component *(T_c 1,350–1,250 K)*	Mg, Si, Cr, Li	Fe, Ni, Co, Pd
Moderately volatile *(T_c 1,230–640 K)*	Mn, P, Na, B, Rb, K, F, Zn	Au, As, Cu, Ag, Ga, Sb, Ge, Sn, Se, Te, S
Highly volatile *(T_c < 640 K)*	Cl, Br, I, Cs, Tl, H, C, N, O, He, Ne, Ar, Kr, Xe	In, Bi, Pb, Hg

Condensation temperature T_c is at a pressure of 10^{-4} bars.

6 Formation of the moderately volatile chalcophiles at 670 K (FeS, with Zn, Pb, and As).
7 Formation of silicates with mineral-bound OH (ca. 430 K; this group includes the hydrated silicates – the amphibole tremolite, serpentine, and chlorite).
8 Formation of ice minerals (ca. 140 K) (to include water ice, solid hydrates of ammonia, methane, and rare gases).
9 A residue made up of permanent gases (gases which under natural conditions will not condense are H_2, He, and Ne).

This condensation scheme provides a valuable framework for understanding the mechanisms behind the formation of the different components found in primitive meteorites and a basis for understanding the differentiation of the Earth. Both of these topics are discussed in subsequent sections of this chapter.

2.3.3 Evidence from Meteorites

Meteorites are extremely important to our understanding of solar system evolution, because, in their most primitive form, they are our most ancient samples of the solar system. As such they provide valuable information about the condensation of the solar nebula from which our solar system formed. Whilst they represent, to date, our most abundant sample of extraterrestrial material, we have no idea how representative this is of the solar nebula material as a whole.

Meteorites, as rocks produced in a solar nebula, have formed through a range of processes, some of which are quite different from those observed on Earth. Thus while igneous differentiation processes and metamorphism are recognized in meteorites, there also other processes operating which are not observed in terrestrial rocks. These include evaporation and condensation events related to melting in a gas-rich medium (as discussed in Section 2.3.2), impacting events, and metal-silicate fractionation.

2.3.3.1 Types of meteorite

Meteorites may be subdivided into two main categories – unmelted meteorites, that is those which come from a parent body which has not been fractionated since its aggregation early in the history of the solar system, and melted, or differentiated meteorites (Fig. 2.8). Unmelted meteorites are stony meteorites, the chondrites, and are made up of the same silicate minerals that are found on Earth. Melted meteorites are of three types. They include some stony meteorites (the achondrites), the iron meteorites, whose composition is dominated by a metallic iron–nickel alloy, and stony-iron meteorites, meteorites which are made up of approximately equal proportions of

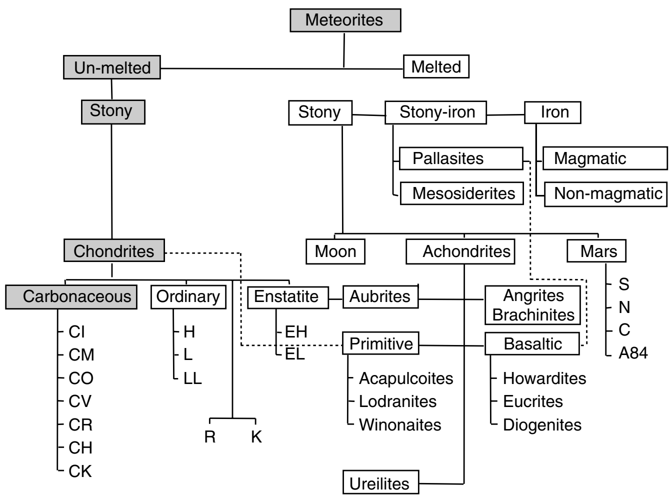

FIGURE 2.8 Meteorite classification from the Natural History Museum of London's *Catalog of Meteorites, Fifth Edition* (Grady, 2000).

silicate minerals and iron–nickel metal (Grady, 2000). Melted meteorites have experienced chemical differentiation during their history and so do not preserve the most primitive matter of the solar system. For this reason much of the discussion which follows will concentrate on the unmelted, chondritic meteorites.

Chondrites. Chondrites are stony meteorites and are the most abundant meteorite type (87% of all meteorites). Their radiometric ages are around 4.56 Ga and these ages are thought to define the time when the solar system formed. Chemically their element abundance patterns, apart from the very light and/or volatile elements, are the same as that of the sun and other stars, and for this reason they are thought to represent undifferentiated cosmic matter. Chondrites therefore are thought to represent the most primitive material in the solar system. They are the "stuff" from which all other rocky materials were built.

Chondrites are ultramafic in composition and contain the minerals olivine, pyroxene, and metallic iron. They are composed of three main components (see Fig. 2.9), each of which represents a different component of primitive solar nebula material:

- Chondrules – spheroidal ultramafic melt droplets a millimeter or so in diameter, which tend to dominate the texture of their host and from which chondrites take their name.
- CAI's – refractory inclusions, or Ca–Al-Inclusions, up to 2 cm across, enriched in Si-poor, Ca–Al-rich minerals. The most abundant source of CAIs is the Allende meteorite, which fell in 1969.
- Matrix – porous, fine grained mineral matter that fills the space between the chondrules and CAIs.

Chondrites are subdivided into carbonaceous (C), ordinary (O), and enstatite (E) varieties (Fig. 2.8). Carbonaceous chondrites are volatile rich and contain abundant carbon in their matrix. Because they have a high volatile content they are thought to be the most primitive of all chondrites. Within this group there are a number of varieties named after type specimens designated CI, CM, CV, etc. An earlier classification used C1 to C3. CI chondrites are the most primitive meteorites within the carbonaceous chondrite groups and the most primitive of all meteorite types. They are the least chemically fractionated and have the highest volatile content. Ordinary chondrites, as their name implies are the most abundant

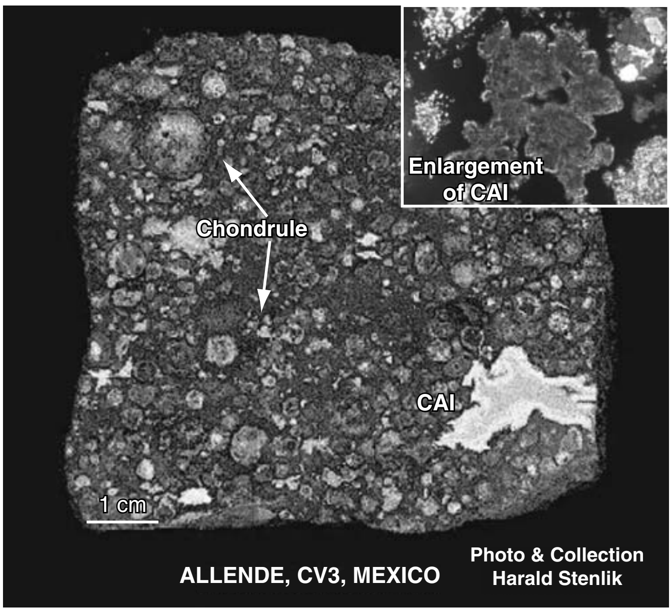

FIGURE 2.9 A slice of the Allende meteorite showing rounded chondrules, a large white CAI and a dark (fine grained) matrix. The inset at the top right shows an enlargement of a CAI in thin section (from http://www.meteorite.com/gallery/allende.htm; photo Harald Stehlik).

of all chondrites. These are subdivided on the basis of their iron content. Enstatite chondrites are highly reduced meteorites and more siliceous so that enstatite rather than olivine is the dominant silicate phase. They are thought to have formed under different redox conditions from other chondrites, probably in a different region of the solar nebula (Kallemeyn & Wasson, 1986).

Achondrites. Achondrites are stony meteorites formed by the melting of their parent body. They are differentiated meteorites which have lost their original metal content. Generally they do not contain chondrules. There are a number of different categories of achondrite representing melted chondrites, basaltic igneous rocks, and planetary regolith breccias.

Iron meteorites. Iron meteorites are thought to be derived from the segregated metallic iron cores of small planetary bodies, which were originally a few tens to hundreds of kilometers in diameter. They demonstrate that metal-silicate fractionation was a fundamental process during the evolution of the solar nebula. Mineralogically they are composed of the minerals kamacite (Fe–Ni metal with a low $< 7\%$ Ni content), and taenite (Fe–Ni metal with a high Ni content, 20–50%). Iron meteorites are subdivided into magmatic irons, iron meteorites that have solidified by fractional crystallization from a melt, and nonmagmatic irons, iron meteorites which do not seem to have completely melted. There is also a chemical classification based upon the concentration of Ge and Ga (Wasson, 1985).

Stony irons. Stony-iron meteorites are those which contain equal proportions of silicate minerals and metallic iron. Pallasites are made up of olivine and Fe–Ni metal and are thought to represent samples from the core–mantle boundary of their parent body. Mesosiderites are brecciated mixtures of silicates and Fe–Ni metal.

Meteorites from other planetary bodies. A small number of lunar meteorites are known. These include anorthositic regolith breccias, basalt, and gabbro. Martian meteorites are identified from their noble gas and oxygen isotope compositions and are known as SNCs (pronounced "snicks") after the three common types – shergottites, nakhlites, and chassignites. Probably the most famous Martian meteorite ALH84001 is in a class of its own and is the only sample to date of very primitive Martian crust with a crystallization age of ca. 4.5 Ga. This meteorite was thought at one time to be the host to fossilized bacteria (see Chapter 6, Section 6.1.3.4).

2.3.3.2 The primitive matter of the solar nebula

Chondrites, the most primitive of all meteorites, formed in dynamic energetic, dust-rich zones in the solar nebula. In this environment, dust/gas ratios were constantly changing, temperatures fluctuated through 1,000 K, with multiple cycles of melting, evaporation, condensation, and aggregation. In addition there were influxes of matter from the interstellar dust and the periodic removal of batches of chondritic material to small planetesimals. In this section we explore how the most primitive materials of the solar system were formed and what they can tell us about processes during the condensation of the solar nebula. These materials include chondrules, refractory inclusions (CAIs), and amoeboid olivine aggregates (AOAs), the oldest component parts of chondritic meteorites.

An approach which has been very fruitful in identifying different regions within the solar nebula environment is the study of oxygen isotopes. Clayton et al. (1976) showed that, on a three isotope $\delta^{17}O$–$\delta^{18}O$ plot, the different classes of meteorites defined distinct groups (Fig. 2.10b). On the basis of these distributions Clayton et al. (1976) made two very important observations. First, that chondritic meteorites have very different oxygen isotope ratios from terrestrial rocks. Second, that chondritic meteorites record the fact that a number of different processes took place within the solar nebula (Fig. 2.10). More recently, Clayton and Mayeda (1999) described in detail the oxygen isotope chemistry of carbonaceous chondrites and showed that they lie on a series of mixing lines (Fig. 2.10). Anhydrous minerals from CAIs define the carbonaceous chondrite anhydrous mixing line (CCAM) with a strongly ^{16}O-enriched end-member. Other chondrites define hydration–alteration mixing lines along which there is mixing between a low-temperature end-member, interpreted to be a ^{16}O-poor fluid, and one of a number of anhydrous starting compositions.

2.3.3.2.1 Chondrules

Chondrules are the principal constituent of many chondritic meteorites (Fig. 2.9) and their formation represents a major, pervasive, high-temperature process in early solar system history (see Zanda (2004) for a recent review). They are made up of silicate, metal, sulfide, and glass phases and in detail show a wide variation in chondrule composition, extending from iron-poor to iron-rich and silica-poor to silica-rich varieties. Some chondrules are composite and show high temperature rims on older cores (Kring, 1991).

There are two possible explanations for the chemical variability of chondules. One emphasizes variations in the mix of precursor solids. In this model compositionally different chondrules reflect different starting materials. Alternatively, chondrules vary in composition because of the chondrule-forming process, and record a reaction between chondrules and the ambient gases. A recent experimental study by Cohen et al. (2004) showed that chondrules do in fact vary in composition as a result of open

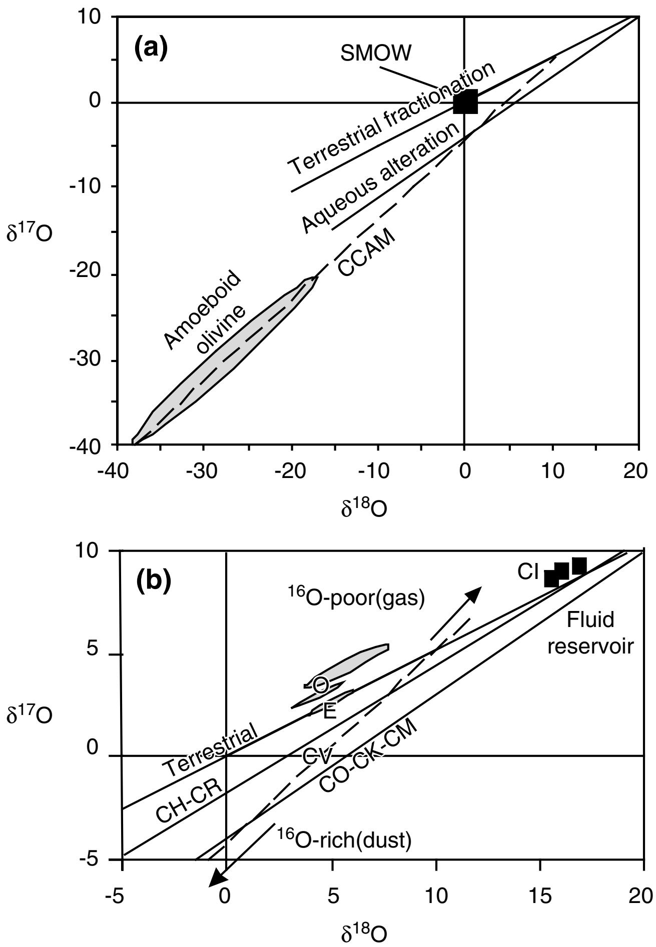

FIGURE 2.10 (a) An oxygen isotope plot for chondritic meteorites showing the two main meteorite trends, relative to the terrestrial mass-dependent fractionation (MDF) trend (which passes through the oxygen isotope standard SMOW). The CCAM line (dashed) represents a mixing line defined by separated minerals from refractory CAI inclusions. Amoeboid olivines plot at the lower ^{16}O-rich end of this line. The aqueous alteration trend is shown in more detail in (b) below. (b) A detail of (a) showing the compositional ranges for the different carbonaceous chondrite groups (CI, CH, CR, CO, CM, CK, CV) and ordinary (O) and enstatite (E) chondrites. The steep carbonaceous chondrite anhydrous mineral line (dashed) is shown to be a mixture of ^{16}O-rich dust and ^{16}O-poor gas. The different carbonaceous chondrites are shown to be the product of the hydrous alteration (^{16}O-poor, fluid reservoir) of two different (CH–CR and CO–CK–CM) anhydrous components (^{16}O-rich). Data from Clayton et al. (1976), Clayton and Mayeda (1999), Fagan et al. (2004) (see Text Box 5.1, Chapter 5).

system processes, implying that it is the nebular environment rather than a difference in starting material that is the principal control on chondrule formation. It is likely therefore, that different chondrule types formed in regions of different chondrule density, which in turn experienced different degrees of evaporative loss.

The precise nature of the chondrule-forming event, the "chondrule factory," is also the subject of some discussion. Some workers favor the formation of chondrules by the direct condensation of the solar nebula gas as a melt. Alternatively, chondrules could be the residues of evaporation. The presence of relict olivine grains in some chondrules (Jones, 1996) argues against a simple condensation model and may imply multiple condensation-evaporation events.

A further important and yet incompletely resolved matter is the nature of the heating event in which chondrules formed. The experimental study of Cohen et al. (2004) shows that chondrules probably formed in a matter of minutes to hours. This implies a flash heating process (Boss, 1998), such as might be caused by shock-heating or lightning strikes in the solar nebula. If this is the case then chondrule melting temperatures represent transient temperatures rather than the ambient temperature of the solar nebula.

2.3.3.2.2 *Ca–Al-rich inclusions*

CAIs in chondritic meteorites contain the refractory minerals melilite, spinel, pyroxene, plagioclase, and perovskite. CAIs formed in a high-temperature part of the solar nebula, where temperatures were above the formation temperature of forsterite (>1,444 K). CAI's are commonly found in carbonaceous chondrites, and more rarely in ordinary and enstatite chondrites. They are also thought to have formed through evaporation and condensation processes in the solar nebula and may be the product of transitory heating events (Wood, 1988). Oxygen isotope studies show that CAIs are characterized by an extreme enrichment in ^{16}O indicating that they formed in an unusual ^{16}O-rich environment in the solar nebula, the origin of which is not resolved (Nittler, 2003). Mixing trends on an $\delta^{17}O - \delta^{18}O$ diagram suggest that there are at least three different primordial oxygen isotope reservoirs recorded in the formation of CAIs (Fig. 2.10b, Young & Russell, 1998; Clayton & Mayeda, 1999). An important recent observation is that CAIs are now known to have formed over a very short time interval (0.05–0.5 Ma) (Bizzarro et al. 2004; Wood, 2004). Wood (2004) has used this short timescale as constraint to infer that they must have formed in young stellar objects with short histories, that is, in stellar objects of Class 0 or Class I, rather than in the longer T Tauri stage (see Section 2.3.1.1).

2.3.3.2.3 *Amoeboid olivine aggregates*

AOAs are irregular objects also found in chondrites and are up to 1 mm long. They comprise granular olivine, intergrown with the refractory phases diopside, anorthite, and spinel, and contain grains of Fe–Ni metal. The presence of olivine indicates that these aggregates formed in the solar nebula at lower temperatures than CAIs, at below the forsterite condensation temperature. However, oxygen isotope studies by Fagan et al. (2004) show that AOAs have an identical ^{16}O enrichment to that found in CAIs (Fig. 2.10). This implies that AOAs and CAIs formed from the same parcel of gas in the same nebular region, but their mineralogical differences suggest that they formed over different temperature intervals (Fagan et al., 2004).

2.3.3.2.4 *The relationship between chondrules, CAIs, and AOAs*

The contrasting mineralogy of CAIs and chondrules indicates that they formed at different nebular temperatures and perhaps in different nebular environments. This is confirmed by oxygen isotope studies which show that there are significant oxygen isotope compositional differences between chondrules and refractory CIAs and AOAs. Chondrules from C and O chondrites also have different oxygen isotope compositions and appear to have formed in different nebular environments. In contrast, CAIs from all chondrite types and AOAs are isotopically similar and share the same range of light-isotopic oxygen rich compositions (Guan et al., 2000).

If AOAs and chondrules originally formed in different nebular environments, how they subsequently came together in chondrites is a problem. CAIs and AOAs, must have formed in a restricted region within the solar nebula and were subsequently dispersed and mixed with chondrules. In part the relationships may be explained in terms of the timing of their formation, as is being revealed by modern high precision isotope measurements. For example, recent Pb isotope studies of chondrules in carbonaceous chondrites show that they formed over a period of about 4 Ma, between 4,563 and 4,567 Ma. CAIs on the other hand are known from ^{26}Al studies (see Text Box 2.3) to have formed slightly earlier than, or at the same time as, chondrules but over a short time interval of < 0.6 Ma, at 4,567 Ma (Amelin et al., 2002, 2004; Bizzarro et al., 2004; Haack et al., 2004). In fact increasingly precise age measurements of chondrules and CAIs suggest multiple melting events within very short time intervals (Krot et al., 2005; Young et al., 2005).

These results suggest that CAIs and chondrules formed in a dynamic solar nebula setting, in which a number of different processes were operating, which we now categorize as chondrule formation. It is likely that large oxygen isotope fluctuations were taking place at this time with O-isotopes compositions varying on a scale of months to years.

2.3.3.3 Presolar matter

The study of presolar matter is one of the growing areas of modern space science. Presolar grains are of great scientific importance because they bring stellar material into the laboratory where it can be directly analyzed and provide much more stringent tests of models for stellar evolution and nucleosynthesis than can be provided by the remote sensing of stellar dust from observational astronomy. It is thought that presolar grains formed in red giant stars, of a type known as asymptotic giant branch (AGB) stars, and in supernovae (Nittler, 2003).

Presolar grains have been identified in both chondritic meteorites, and in interplanetary dust particles (IDPs) collected from the Earth's stratosphere. They are identified by their rare gas isotopic signature which is different from that which characterizes our solar system. This unusual isotopic signature implies their genesis in a different stellar environment, outside of the solar system. This previous history means that these grains formed before the solar system began, and traversed interstellar space prior to their incorporation into the solar nebula. "Each grain is a frozen piece of a single star which ended its life before the formation of the solar system" (Nittler, 2003). The grains are normally extremely small, about 1 μm, and are only found in meteorites if they are subjected to extensive acid dissolution – a process which has been likened to burning a haystack in order to find the needle. Even then, their extrasolar character can only be recognized after detailed isotopic examination by ion probe.

2.3.3.3.1 Presolar grains in meteorite residues

Presolar grains are found in carbonaceous chondrites and include graphite spherules, organic carbon, nano-diamond, silicon carbide, and a range of other metal carbides. More rarely there are grains of silicon nitride and the oxides corundum, spinel, and the phase hibonite (a Ca–Al-oxide) (Nittler, 2003; Zinner et al., 2003). Phases such as corundum, hibonite, and spinel are phases which are expected to condense first in a gas of solar composition. The presence of these phases as presolar grains indicates that their stellar sources have a similar condensation sequence to that of the solar nebulae outlined in Section 2.3.2.1. In detail, presolar grains tend to have very variable isotopic compositions implying that they have been derived from many different stellar environments (Zinner et al., 2003).

2.3.3.3.2 Interplanetary dust particles

IDPs collected in the Earth's stratosphere are of multiple origins. Solar system objects come in anhydrous and hydrated forms. The anhydrous, chondritic-porous group are thought to be the most primitive and least-processed of all matter in the solar system and are probably of cometary origin. Hydrated IDPs, on the other hand, are linked to an asteroid origin (Keller et al., 2004).

IDPs of presolar origin are also abundant in stratospheric dust and include silicate-rich and carbon-rich grains. Currently the only silicates observed are forsteritic olivine and a glass embedded with metal and sulfide (GEMS) (Messenger et al., 2003). Some organic molecules have a D- and N-isotopic signature which can only be explained by their origin in a very low-temperature molecular cloud (Keller et al., 2004) and provide important insights into the nucleosynthetic processes which take place within this environment.

2.3.4 Planetary formation

The final stage in the condensation of a solar nebula is that of planetary formation. Planets are thought to form in a protoplanetary disk of the type observed around young stellar objects such as Beta Pictoris (Section 2.3.1.1). The lifetime of such dust-laden protoplanetary disks is of the order of 10^7 years. Until recently we knew very little about processes operating in such protoplanetary disks, and much of what we did know was drawn from the study of the solar system. However, the recent discovery of planetary systems around other stars suggest that our solar system may not be characteristic of planetary systems in general and many new advances can be expected in this field.

2.3.4.1 The standard model of planetary formation

Wetherill (1990) has provided the standard model of planetary formation, based upon the planetesimal hypothesis. This model states that planets grow within a circumstellar disk, via pairwise accretion of smaller bodies known as planetesimals. It should be noted that the process of planet formation is a fundamentally different process from that of star formation. Stellar formation begins with the process of gas condensation, whereas planetary formation begins with the accumulation of solid bodies, and gas accretion takes place only at a late stage in some of the larger planets (Lissauer, 1993).

In order to be successful, it is necessary that the standard model of planetary formation should explain the main features of the solar system, in particular the division of the planets into three main groups – the terrestrial planets, the giant planets and the outer icy planets (Table 2.2). In detail the standard model should also explain the following properties of the solar system (Lissauer, 1993):

- the coplanar nature and spacing of the planetary orbits;
- the presence of cometary reservoirs in the Kuiper belt at ca. 40 AU, and beyond in the Oort cloud, at 10000 AU;

TABLE 2.2 Physical properties of the planets showing the three groups of planets. The Asteroids lie between Mars and Jupiter at 2.7 AU.

		The terrestrial planets				The giant planets		The outer icy planets		
Body	**Sun**	**Mercury**	**Venus**	**Earth**	**Mars**	**Jupiter**	**Saturn**	**Uranus**	**Neptune**	**Pluto**
Increasing mean distance from Sun (Earth to Sun = 1.0 AU)										
Distance from the sun (AU)	0	0.39	0.72	1	1.52	5.2	9.55	19.2	30.1	39.5
Mean density (Terrestrial planets > Jovian planets)										
Actual Density ($g\ cm^{-3}$)	1.41	5.43	5.25	5.52	3.95	1.33	0.69	1.29	1.64	2.03
Radius (Terrestrial planets < Jovian planets)										
Radius (Earth = 1.0)	109	0.38	0.95	1	0.53	11	9	4	4	0.18

- the existence of satellite systems for most planets;
- the variation in planetary masses, from the relatively small terrestrial planets to the large gaseous planets;
- the concentration of the majority of the angular momentum of the solar system in the planets, despite these representing only a small fraction of its total mass;
- the variable bulk compositions of the dense, refractory, terrestrial planets, the low density giant planets, and the icy outer planets;
- the existence of the asteroid belt and meteorites;
- the record of dense cratering on most solid planetary and satellite surfaces.

The processes of cosmochemistry constrain planetary materials to be one of three types – gas (hydrogen and helium – the most abundant elements of the Universe), ice (water, methane, ammonia, nitrogen – the next most abundant elements in nucleosynthesis), and rock – principally made up of Mg–Fe silicates (Stevenson, 2004). If the standard model of planetary formation is applied to the formation of the Earth and the terrestrial planets, then temperatures in the solar nebula in the vicinity of the Earth's orbit would have been between 500 and 800 K. At these temperatures rock – Fe–Mg silicates, and Fe–Ni metal would condense but not water ice. Micron-sized particles of these minerals would have grown in series of stages into the present configuration of planetary bodies as outlined below and summarized in Table 2.3.

2.3.4.1.1 Stage 1. The formation of small (1–10 km) planetesimals

The first stage of planetary formation involves the accumulation of micron-sized dust particles into kilometer-sized, 10^{12}–10^{18} g, planetesimals, over a timescale of 10^4 years. Small grains in the solar nebula settle toward the midplane of the nebula, where they are buoyant in the radial gas pressure, and accumulate largely through nongravitational, electromagnetic forces, such as weak Van der Waal's binding energies. Recent observations of protoplanetary disks has confirmed the existence of these materials in the "terrestrial region" of the disk (Van Boekel et al., 2004).

2.3.4.1.2 Stage 2. Gravitational accumulation of planetesimals into planetary embryos

When planetesimals grow to radii of between 0.1 and 10 km the nongravitational accumulation growth stage come to an end. At this stage the relative velocities of these larger bodies is their key property and subsequent processes become dominated by mutual gravitational perturbations. Hence there is a transition from nongravitational accumulation to gravitational accumulation. It is through this process that planetary embryos, or protoplanets as they are also called, up to 4,000 km in size (10^{26}–10^{27} g, Mercury- or Mars-sized), are formed. Our understanding of protoplanet formation has been greatly aided by mathematical simulations, a technique pioneered by Wetherill (1990). A more recent simulation by Weidenschilling et al. (1997) found that the distribution of planetesimals within the orbits of Mercury to Mars reduced to 22 planetary embryos, with masses of $> 10^{26}$ g, over 10^6 years. Together these bodies represented 90% of the total mass. The accretion process ceases when the supply of suitably sized, locally available material is exhausted.

TABLE 2.3 Stages of planetary formation according to the "standard model" (Wetherill, 1990), applied to the terrestrial planets.

Stage	Final mass (g)	Time taken (yr)	Main processes
1. Accretion of dust-sized particles into planetesimals.	10^{12}–10^{18}	10^4	Nongravitational accumulation; particles coalesce through electrostatic forces
2. Accretion of planetesimals into planetary embryos	10^{26}–10^{27}	10^6	Gravitational accretion aided by runaway growth
3. Accretion of planetary embryos into planets	10^{27}–10^{28}	10^7–10^8	Giant impacts

2.3.4.1.3 Stage 3. From embryos to planets

The final stage of planetary accretion is the accumulation of a few tens of planetary embryos into a small number of full-sized planets, 10^{27}–10^{28} g, over a timescale of 10^7–10^8 years. There are two processes which appear to be important at this stage. The first is the very high probability of giant impacts between planetary embryos. The importance of giant impacts was first postulated by Wetherill (1990) on the basis of his numerical simulation experiments. Giant impacting will almost inevitably lead to planet-scale melting and in some cases to planetary disintegration (Asphaug et al., 2006). The second key process in the final assembly of planets is the dispersion of the gaseous component of the solar nebula. This is thought to have happened on the time scale of 10^6–10^7 years (Canup, 2004). The loss of the gaseous component would reduce the velocity damping on small objects, which would in turn reduce their ability to damp the velocities of the planetary embryos, leading to collisions, and, as indicated above, giant impacts. The noble gas geochemistry of the Earth's mantle indicates that the Earth has retained a memory of the solar nebular gas (see Chapter 5, Section 5.2.1.4). This must have been acquired in the first 10^6–10^7 years of its accretion history.

2.3.4.2 The formation of giant (gaseous) planets

According to the standard model, the giant gaseous, or Jovian-type planets form in a different manner from the terrestrial planets. They have a rocky core, a gaseous outer layer, and may have a middle layer rich in ice, possible because of their greater distance from the sun and lower nebular temperature (Fig. 2.6). Their outer gaseous layer is thought to be captured gas from the solar nebula.

Models for the formation of the giant planets suggest that a rocky planetary embryo of about ten Earth masses can form rapidly, within 10^6 years. Once this embryo is established these massive planetary embryos accumulate two Earth masses of solar nebular gas over 10^7 yr (Kortenkamp et al., 2001).

More recently our understanding of the nature of the giant gaseous planets has been challenged by the discovery of planetary systems around other stars (Lissauer, 2002). Many of these "extrasolar" planets are giant gaseous planets, but with rather unusual properties, for many are less than 0.1 AU away from their parent star, unlike Jupiter's 5 AU. In part this is an observational bias given that large giant planets close to their parent stars are more readily detectable. Observations of extrasolar, Jupiter-like planets have led to an alternative model for their formation, whereby they form by disc instability, through the rapid (100 years) gravitational collapse of clumps of dust and gas in the protoplanetary disk (Boss, 2000). At present however, the consensus seems to favor the "rocky core" nucleation model (Stevenson, 2004).

2.4 Earth differentiation – the first Earth system

It is most likely that the Earth formed according to the standard model of planetary accretion, as described in the previous section. Given this assumption, the earliest Earth system is likely to have had the following properties:

- *A chondritic composition*. The Earth formed from the primitive materials of the solar nebula, which, apart from the volatile elements, is identical to that of primitive chondritic meteorites. It is likely, therefore, that the initial bulk composition of the Earth was chondritic.
- *The Earth experienced one or more giant impacts*. Given that giant impacting is an essential part of planetary accretion models for the terrestrial planets, leading to planet-wide melting, it is probable that the Earth experienced one or more planet-wide melting events during its earliest history.
- *Formation of a terrestrial magma ocean*. Extensive melting as a result of giant impacts would lead to the formation of a terrestrial magma ocean during the Earth's late accretion history.
- *Extensive melting may have facilitated core formation*. It is probable that during its magma

ocean stage the Earth differentiated into an outer silicate mantle and an inner metallic core.

- *The Moon formed through a giant impact*. It is now thought likely that the Moon formed as a result of a giant impact event. The timing of this event, its contribution to terrestrial melting, and the bulk composition of the Earth are important subjects of current research.

However, the standard planetary accretion model also raises a number of questions about the early Earth. For example:

- *How do we define the age of the Earth?* If the Earth formed by accretion, over a time period of 10–100 million years, at what stage of this process do we attribute the age of the Earth?
- *To what extent were the planetesimals and protoplanets, from which the Earth was built, already differentiated?* Early models for the formation of the Earth assumed that it formed from undifferentiated starting materials. This is not necessarily the case and the Earth may have formed from protoplanets which already possessed their own metallic core.
- *What sort of early crust formed on Earth?* And is it still preserved? This topic is discussed more fully in Chapter 3 (Section 3.2.3.5).

Our purpose in this section is to seek an understanding of the earliest differentiation of the Earth and how the Earth acquired its large-scale layered structure of core, mantle, and atmosphere-oceans. A major result of "planetary thinking" about the early Earth is that we now recognize that several large-scale features of the Earth may all be linked to giant impacting events. These include the formation of the Moon, the existence of a magma ocean, and the separation of the core. Whether or not these are all the result of a single event or many is the subject of some discussion (Kleine et al., 2004).

2.4.1 The formation of the Moon

The standard model for the formation of the Moon is the Giant Impact hypothesis (Stevenson, 1987). This model proposes that a planetesimal, the mass of Mars (about 15% the mass of the Earth), collided with the proto-Earth, at a time after core formation. The impact generated a huge amount of thermal energy so that the impactor and part of the Earth were vaporized, and some of this material coalesced in an orbit around the Earth to form the Moon. On cooling it is widely thought that both the Earth and the Moon went through magma ocean stages (see Section 2.4.3).

2.4.1.1 Modeling the Giant Impact

Particular insights into the Giant Impact process have been gained through the application of numerical modeling. Melosh (2001) points out, however, that such an approach is not for the faint hearted, and that "it has taken squadrons of physicists nearly 50 years to come up with computers and three-dimensional computer codes that can adequately treat the effects of impacts and explosions under relatively simple conditions." Over the past decade or so, numerical solutions to the Giant Impact event have cycled through the more and less probable. At present a probable (and mathematically sophisticated) solution is proposed by Canup and Asphaug (2001) in which they find that an impactor, the mass of Mars (with a mass of ~6×10^{26} g), collided at an oblique angle with an almost fully formed Earth to produce an iron-poor Moon. The impactor has been named "Theia," after the mother of the Greek goddess of the Moon (Halliday, 2000).

In detail, an impact of this type, starting with two bodies both with iron cores and silicate mantles, would result in a planet surrounded by a disk of former mantle material. It is from this disk that an iron-depleted Moon would accrete (Canup, 2004). Models of this type are proving highly successful inasmuch as they have the capacity to simultaneously explain the masses of the Earth and Moon, the Earth–Moon angular momentum, and the unusual chemical composition of the Moon.

2.4.1.2 Geochemical tests of the Giant Impact model

Returned lunar basalt samples presented a few surprises when their chemical compositions were first determined, for their chemistry turned out to be rather different from their terrestrial counterparts. Particular chemical features of lunar basalts are their strong depletion in highly volatile elements (Fig. 2.11), and modest depletion of moderately volatile elements, relative to the Earth's mantle.

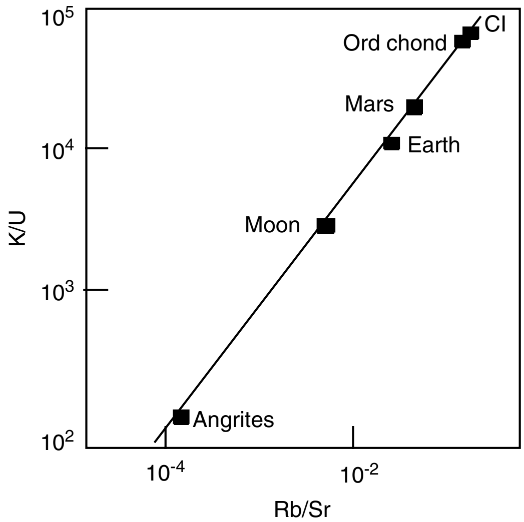

FIGURE 2.11 The ratio of volatile (K, Rb) to refractory elements (U, Sr) in planetary and solar system objects (after Halliday & Porcelli, 2001). The relationships show the volatile depleted nature of the Moon relative to the Earth and the Moon and the Earth relative to primitive CI chondrites.

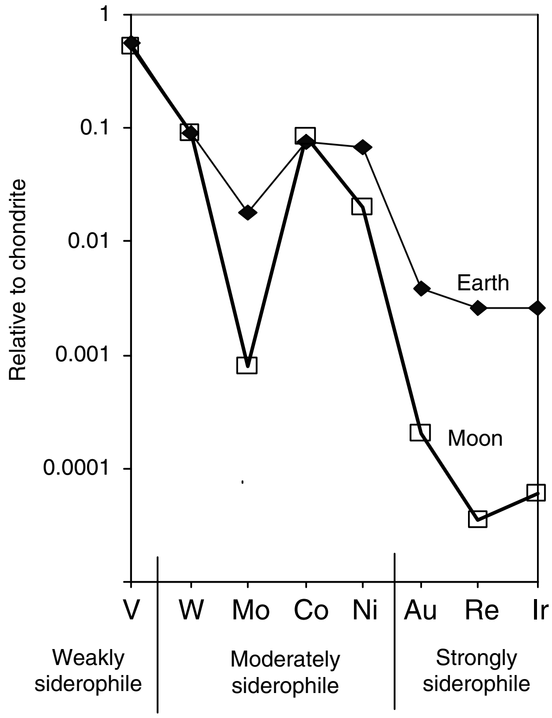

FIGURE 2.12 Depletion factors for siderophile elements in the Earth's mantle and the Moon relative to C1 chondrite, using the median Earth and Moon values from the compilation of Kramers (1998) (see Text Box 2.2).

The Moon also has an unusually low iron content. Typical inner solar system objects contain about 30% iron – CI chondrites, for example contain about 36% iron by mass – whereas the Moon contains only 13 wt%. Some of this iron is probably located in the lunar core, although this will only account for a small amount of iron, since the lunar core is small (3–4% of its mass) compared to that of the Earth. In contrast the more refractory lithophile elements such as Al are more abundant on the Moon given the thick aluminous lunar crust (Taylor, 1987).

Jones and Hood (1990) approached the problem of the lunar composition by assuming that it had the same composition as the Earth's mantle. They showed that if this were the case then it would also have had a large metallic core. However, the Moon does not have a large metallic core and by this logic cannot be made of the same material as the terrestrial mantle. A solution to this paradox was proposed by Kramers (1998) who showed that siderophile element patterns for the silicate Moon are similar to the terrestrial pattern for some elements but are more strongly depleted for others (Fig. 2.12). This model suggests that the Moon formed from an already differentiated body, but was depleted further during lunar core formation (Kramers, 1998).

Very high precision oxygen isotope studies show that, within the limits of analytical error, the Earth and the Moon have identical isotopic compositions. Oxygen isotope studies of meteorites summarized in Fig. 2.10, show that the inner solar system was isotopically heterogeneous, and so the Earth–Moon result implies that the proto-Earth and the impactor Theia must have accreted at a similar distance from the sun and grew from a similar mix of materials (Wiechert et al., 2001). One implication of this finding is that the chemical differences between the Earth and Moon described above may be of a secondary origin, in the sense that they were produced during the differentiation of the Earth, Theia, and the Moon.

2.4.1.3 Consequences of a Giant Impact for the Earth
The likely implications of the Giant Impact hypothesis for the early Earth are that:
- About 30% of the planet's mass would be raised to temperatures greater than 7,000 K, so that the Earth would be surrounded by a silicate vapor atmosphere. In addition much of the planet would have been in a molten state.
- The Earth's atmosphere would have been volatilized, either at impact or during the magma ocean stage, although in the case of an oblique impact, the atmosphere may have condensed back again.
- It is also possible that, if the impactor had a metallic core of its own, this was added to the Earth's core immediately following the impact (Benz & Cameron, 1990).

The Earth however is a dynamic planet, with a convecting mantle, and identifying evidence for these events in the modern Earth's mantle has proved an elusive task, as will be shown below.

2.4.1.4 The timing of the impact
The oldest rock on the Moon is a clast of ferroan anorthosite in an impact breccia which has a relatively imprecise Sm–Nd isochron age of 4,562 ± 68 Ma (Alibert et al., 1994). Tungsten isotope measurements (see Section 2.4.2.5) on lunar rocks indicate that the Moon formed about 30 Ma after the formation of the solar system (Schoenberg et al., 2002). Halliday (2004) suggested that the Moon is younger and formed > 44 Ma to > 54 Ma after the beginning of the solar system, but the consensus view is that the timescale of planetary accretion was relatively short and that the Moon formed within the first 30 Ma of the life of the solar system (Kleine et al., 2002; 2005b; Yin et al., 2002). In fact the tungsten isotope data are now sufficiently good to allow us to discriminate between competing impactor models (Jacobsen, 2005) Kleine et al., 2004 and confirm the model of Canup and Asphaug (2001) in which a Mars-sized impactor collided with an almost fully formed Earth. Thus the process of terrestrial accretion had ceased by about 30 Ma and was in fact terminated by the Moon-forming impact.

2.4.2 Core formation
Geophysical evidence shows that the Earth has a liquid Fe–Ni–S-alloy outer core with a thickness of 2,260 km, and a solid Fe–Ni-alloy inner core, with a radius of 1,215 km. Temperatures at the top of the core are thought to be in the range 3,500–4,500 K and rise to 5,000–6,000 K at the center of the Earth. There is a mismatch of a few percent between the measured density of the Earth's outer core and that predicted for an iron–nickel alloy at high pressure. This "core density deficit," as it is called, is thought to indicate the presence of other elements as impurities in the core in addition to iron and nickel, and this could be the principal reason why the outer core is molten. The impurities act as a form of "antifreeze" in the liquid metal (Stevenson, 1990).

At the present day the Earth's inner core continues to grow at the expense of the outer core and this process generates heat in the modern Earth. Estimates of this heat flux are not well constrained and vary from 2 TW to 10 TW (Labrosse, 2002). The Earth's magnetic field is thought to be driven by a geomagnetic dynamo, which is thought to be governed by thermal convection in the outer core. The driver for this thermal convection is not well understood and could be radioactive heating (if potassium is present in the core), the cooling of the core, or the latent heat arising from crystallization at the inner/outer core boundary. Weak paleointensity measurements of the Earth's magnetic field have been recorded in rocks as old as 3.5 Ga (Yoshihara & Hamano, 2004).

2.4.2.1 Impurities in the Earth's core
Birch (1952) demonstrated that the Earth's liquid outer core is 10% less dense than expected if it were made up of an iron–nickel alloy. For this reason one or more light elements are thought to be present in the core. Although a core density deficit of 10% has been widely used in many geochemical studies this value has recently been revised downwards by Anderson and Isaak (2002) and is now thought to be 5.4%.

A suitable light element diluent must be able to form an alloy with Fe at core pressures,

TEXT BOX 2.2 Geochemical multielement diagrams

Geochemists use a variety of trace element diagrams in which to display multielement data. These take a variety of forms but have some features in common. Typically a multielement diagram will display a range of trace elements equally spaced along the x-axis of the diagram and these will be arranged in a specific order according to the particular logic of the diagram. The y-axis will record the abundances of those elements, and because the abundances are very variable, they are displayed on a logarithmic scale. Further, the abundances are normalized to the concentrations present in a particular reference material. These reference materials vary but include chondritic meteorites and an estimate of the composition of the Earth's primitive mantle. In other words, the composition of the rock is compared to that of the primitive, undifferentiated Earth. Three different types of multielement diagrams will be discussed here.

Rare Earth element (REE) diagrams

The REEs are the lanthanides, elements 57 to 71 (La to Lu) in the periodic table. They are of particular interest because geochemically they are very similar. All carry a 3+ charge and they show decreasing ionic radii from La to Lu. They are expected therefore to behave as a coherent group and to show smooth, systematic changes in geochemical behavior through the series. Hence REE diagrams are plotted to show the elements of the group in order of increasing atomic numbers (from La (57) to Lu (71)) from left to right. REE concentration in rocks are normalized to the concentrations in chondritic meteorites and there are a number of recommended chondrite concentrations in use. One widely used set of chondritic normalization values is that of McDonough and Sun (1995) reported in Chapter 3, Table 3.2. The purpose of this normalization is to compare samples with the compositions of the original starting material of the Earth.

Of interest is the extent to which the REE vary within the group. Where there are trends of increasing or decreasing abundances within the group the origin of this "fractionation" is of interest and comparisons are made between the light (lower atomic number) and heavy (higher atomic number) members of the group (Box 2.2 Fig.1). Where single elements have abundances which are atypical, the origin of these "anomalies" is of interest.

REE plots have been widely used to understand magmatic processes in igneous rocks, but have also been useful in unraveling sedimentary processes and geochemical exchanges in seawater (see Chapter 5, Section 5.4.2).

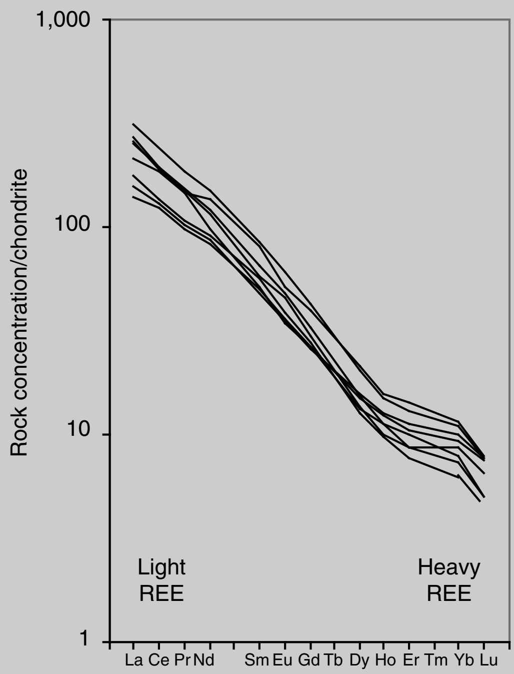

BOX 2.2 FIGURE 1 An REE plot for granitoids from the Baltic Shield, showing the REEs in order of their atomic number on the x-axis and concentrations, normalized relative to abundances in chondritic meteorites, shown on the y-axis, using a log scale. The graph shows that in these rocks all the REE have higher concentrations than in chondritic meteorites (all values > 1.0) but that the light REE (low atomic number, at the left) have much higher abundances than the heavy REE (higher atomic number, at the right). The reason for this "fractionation" is important to determine.

Multi-trace element diagrams

Multielement diagrams are quite variable and care needs to be taken to identify which set of normalizing values are being used. Clearly this will vary according to the purpose of the diagram. Multielement diagrams have also been known as "spider diagrams", because the apparently chaotic abundance patterns that they sometimes generate resemble the track of a spider walking through ink!

(a) Primitive mantle-normalized plots

A primitive mantle normalized trace element diagram appears to use a rather random set of trace elements.

The series will often start with elements such as Cs or Rb and end with elements such as Y or Yb, although there is no definitive element suite for these diagrams. In this case the elements are not ordered according to atomic number, instead they are arranged in order of decreasing incompatibility during mantle melting. In other words those elements with the greatest preference for the melt phase during mantle melting are plotted to the left of the graph and those with a lesser affinity for the melt phase to the right (Box 2.2 Fig.2). These preferences are determined from laboratory measurements of the partition coefficients of the respective elements in the main mantle minerals, weighted according to the proportion of those minerals in the mantle. These abundances are normalized to the concentrations of those elements estimated to have been present in the Earth's primitive mantle – that is the mantle as it was after core formation but before the formation of the continental crust. A table of the various estimates of these abundances is given in Chapter 3, Table 3.2. Hence the purpose of this normalization procedure is to see how the sample being investigated differs from the primitive mantle from which it was originally derived.

(b) Mid Ocean Ridge Basalt (MORB)-normalized diagrams

An alternative normalization scheme is to use the composition of average midocean ridge basalts (MORB). MORB-normalization is often used for volcanic arc rocks and altered basalts. In this case the elements are arranged slightly differently and are ordered according to their mobility in a hydrous fluid so that mobile, low field strength elements are plotted to the left of the diagram and immobile, high field strength elements to the right (Box 2.2 Fig. 3).

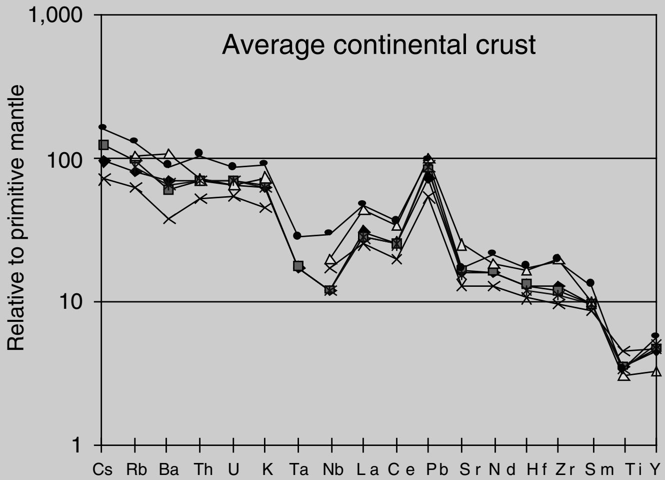

BOX 2.2 FIGURE 2 A mantle-normalized multielement plot for selected trace elements in average continental crust (five different averages). The elements are arranged in order of decreasing incompatibility during mantle melting. The plot shows that all the elements shown are concentrated in the continental crust relative to the primitive mantle but that the highly incompatible elements are highly concentrated (×100) compared with elements such as Ti and Y (×3). Understanding this fractionation is important. Also of interest are the anomalies for Pb and Ta–Nb. For further discussion see Chapter 4, Section 4.2.2.3.

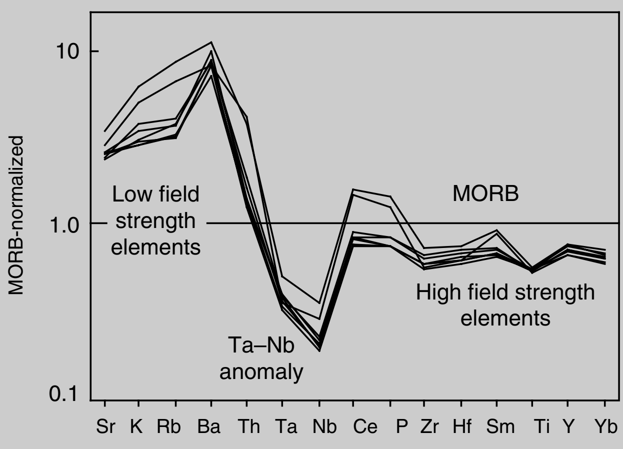

BOX 2.2 FIGURE 3 A MORB-normalized plot for typical arc magmas. This normalization procedure highlights the differences between fluid-mobile elements (the low field strength elements) and immobile elements (the high field strength elements). Fluid-mobile elements have higher concentrations than average MORB, whereas the immobile elements have (in this case) lower concentrations than in average MORB. For further discussion see Chapter 4, Section 4.1.2.

TEXT BOX 2.2 (*Cont'd*)

Siderophile element diagrams

The siderophile elements are those which have a strong affinity for metallic iron. These are the elements therefore that preferentially partition into the Earth's core during planetary formation. Understanding the distribution of the siderophile element concentration in the Earth's mantle can provide important clues about the origin of the Earth's core. There are a range of different siderophile element diagrams using different groups of siderophile elements. The features that they have in common are that they order the siderophile elements according to their siderophile affinity. This is normally in order of increasing siderophile nature from left to right. Concentrations are normalized according to abundances in chondritic meteorites (Box 2.2 Fig. 4) (see Section 2.4).

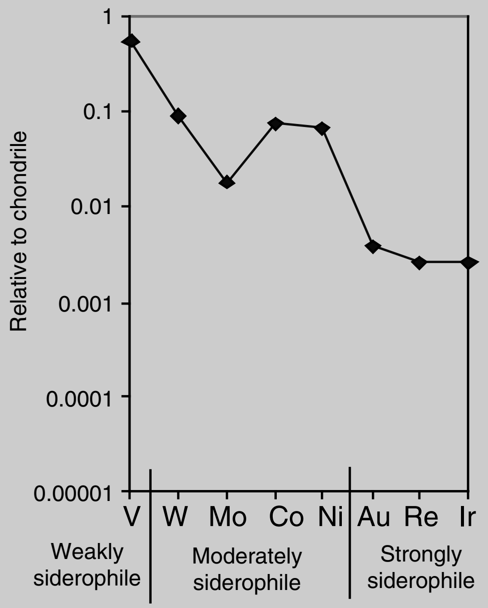

BOX 2.2 FIGURE 4 A chondrite normalized plot for siderophile elements in the Earth's mantle. The elements are arranged in order of increasing siderophile affinity from left to right and show decreasing element abundances with increasing siderophile character, commensurate with core formation.

partition into the core in sufficient quantity, and form an alloy that matches the known seismic properties and density of the outer core. Identifying precisely the appropriate light elements in the core is likely to provide important clues to the process of core formation, as discussed below (Section 2.4.2.4.2). Over the years a large number of elements have been proposed as candidates for the light element contribution in the core, the current contenders being O, Si, and S (Williams & Knittle, 1997). The key lines of evidence in their support are summarized in Table 2.4.

2.4.2.2 The mechanism of core formation

The principal constraint on the formation of the Earth's core is that the Earth must have been sufficiently molten for metal droplets to separate and sink through a silicate melt (Walter & Tronnes, 2004). Experimental studies show that molten iron alloys cannot migrate along the grain boundaries of solid silicates and silicate-metal separation only effectively takes place in a melt. Given this starting point a large number of questions arise about the details of core formation. For example:

- Had the planetary bodies from which the Earth accreted already melted and so acquired their own cores?
- In other words, was the equilibration between silicate and melt primarily a low pressure process (in small bodies – planetesimals or protoplanets) or a high pressure-high temperature process in an almost fully accreted Earth?
- Did chemical equilibrium exist between the silicate and metallic components of the early Earth during core formation?
- For example, if small bodies with metallic cores merged during accretion did they do so without equilibration with the silicate mantles, or was there large-scale melting and rehomogenization?
- To what extent did the Moon-forming impact drive the process of core formation?

Some consensus is now emerging on the process of core formation through an exploration of the likely heat sources for the melting during which silicate and metal can separate, from geochemical constraints based upon the siderophile elements, and from our knowledge of the timing of core formation,

TABLE 2.4 Competing models for the likely light element diluents in a Fe–Ni-rich outer core.

Light element	Approximate %	Evidence	Reference
Sulfur	<6 wt%	FeS forms eutectic properties with Fe, S is commonly found in Fe-meteorites as FeS (Troilite) 2–15 wt%	O'Neill et al. (1998)
	2–15 wt%	Layering absent in outer core	Helffrich and Kaneshima (2004)
	>1 % (atomic) (*Inner core*)	Experimental study of Fe–S system near the pure iron end-member	Li et al. (2001)
Oxygen	25–30 mol% Oxygen	High solubility of O in Fe metal. FeO at core pressure is miscible with Fe. O may be essential for compositional convection May imply an oxidized chondritic starting material May be a product of reaction with the mantle through time	Abe et al. (1999) Alfe et al. (2002)
	<6 ± 1 wt%	Layering absent in outer core	Helffrich and Kaneshima (2004)
Silicon	<0.01 wt%	If at low pressure and fO_2	Gessmann et al. (2001)
	<0.1 wt%	High pressure, low fO_2	Malavergne et al. (2004)
	Up to 17%	High pressure – only permissible if very low fO_2	
	5–7%	High pressure – progressive oxidation during accretion	Wade and Wood (2005)
Potassium	250 ppm (could account for 20% of the heat production of the core)	K and Na concentrations in the silicate Earth ~20% less than in C1 chondrites. Either, lost during accretion or, due to K extraction into a S-rich O-rich Fe liquid in the Earth's core	Gessmann and Wood (2002)
Carbon	ca. 1%	Stable as Fe_3C	Wood (1993)

based principally upon the study of tungsten isotopes.

2.4.2.3 Constraints on core formation

2.4.2.3.1 Thermal constraints

Probably the most important source of heat during the early stages of planetary accretion was from the decay of short lived isotopes, in particular ^{26}Al (Walter & Tronnes, 2004). Baker et al. (2005) recently reported isotopic evidence for planetismal melting and differentiation very early in the history of the solar system, triggered by ^{26}Al decay.

Later in the history of planetary accretion, impact melting became a more important source of thermal energy, leading to the creation of magma oceans. On the Earth, a particularly important impacting event – the formation of the Moon – probably led to widespread melting at about 30 Ma. An extreme impact melting event, or events, would lead to extensive melting, homogenization of discrete metal and silicate phases present in the initial accretionary components, and the formation of a magma ocean in which silicate and metallic phases separate, leading to the formation of the Earth's core and mantle.

2.4.2.3.2 Geochemical constraints

The siderophile elements provide an important control on the processes of core formation. Siderophile elements are those elements which have a chemical affinity for metallic iron (Section 2.3.2) and so might be expected to concentrate in the core. This is in fact what is observed, and siderophile element concentrations in the mantle are depleted relative to concentrations in chondritic meteorites, with the "missing" component presumed to be in the core.

However, when calculations are made to compare the measured siderophile element depletion in the mantle with the expected values, there is a mismatch. Using metal–silicate partition coefficients measured at low pressures and temperatures, it was found that the depletion is not as great as is expected (Fig. 2.13). For some elements the depletion is several orders of magnitude less than that expected after core formation. This problem, first noted by Ringwood (1966) for the elements Ni and Co, and subsequently extended to other siderophile elements, has become known as the "excess siderophile problem."

2.4.2.4 Models of core formation

Explanations of the excess siderophile element problem have led to a number of different models of core formation. For example it is possible that the partitioning of siderophile elements between silicate melt and metal alloy was not an equilibrium process. Second, the assumption that silicate–metal equilibration took place at low temperatures and pressures may be incorrect, and high-pressure partition coefficients may be more appropriate. A third possibility is that core formation was complete before the end of accretion and that some siderophile elements were added late in the accretion process of Earth, after the separation of the core and mantle. In this case the mantle was "topped up" with a late addition of siderophile elements.

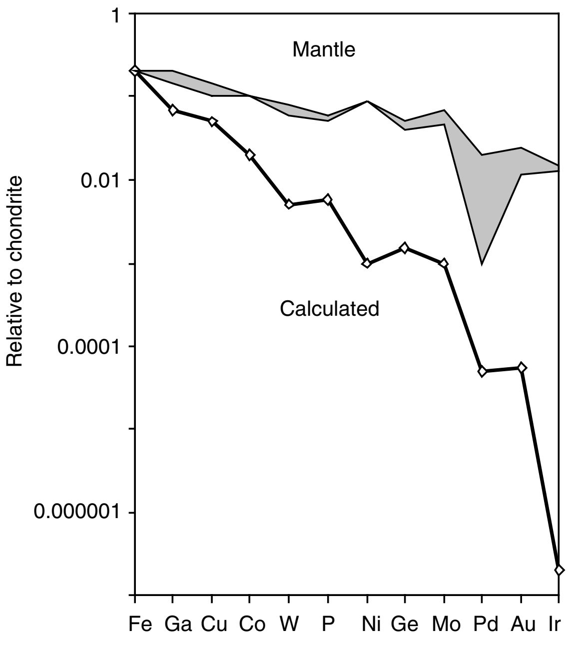

FIGURE 2.13 Chondrite normalized concentrations of siderophile elements in the Earth's mantle relative to those expected in the mantle if all the iron in the Earth's core had equilibrated with silicate at low pressures and temperature. The siderophile elements are arranged such that their siderophile nature increases from left to right (after Rama Murthy and Karato, 1997).

2.4.2.4.1 The low pressure core segregation model

Azbel et al. (1993) and Kramers (1998) proposed that core formation began when the Earth was only 10% formed and took place in a shallow (6 GPa) magma ocean. In this model, protoplanets had already formed cores, which, on impacting, merged without fully equilibrating with the silicate mantle. Hence siderophile element extraction from the mantle was an inefficient process, incompletely scavenging the siderophile elements. This solution to the excess siderophile element problem implicitly accepts that there was not a simple equilibrium relationship between the metallic and silicate components of the Earth during core formation. Kramers (1998) modeled the distribution of siderophile elements on Earth and in the Moon and showed that there are large differences in the extent of depletion from the modest depletion of weakly siderophile elements such as V, to a greater depletion of the moderately siderophile elements (W, Co, Ni, and Mo) to the extensive depletion of the highly siderophile elements (Au, Re, Ir) (Fig. 2.12). This pattern is broadly consistent with low pressure silicate–metal partition coefficients for the siderophile elements and is the pattern expected in the Earth's mantle as a consequence of inefficient metal extraction during core formation.

However, recent modeling by Canup (2004) shows that when there is impacting between bodies with existing metallic cores there will be a general homogenization of silicate and melt and the metallic cores will reequilibrate within a magma ocean.

2.4.2.4.2 The "late veneer" model

The "late veneer" solution to the excess siderophile element problem proposes that there was an initial major accretion event during which the core formed and siderophile elements were removed from the mantle to the core. This was followed by a later stage of accretion during which more oxidizing material was added to the Earth, making up about 7% of the Earth's mass. This contributed to the moderately siderophile element budget of the mantle. Finally, a "late veneer" was added to the Earth representing about 1% of the Earth's mass. Most of the mantle's highly siderophile element content was added at this stage (Newsom & Jones, 1990). The principal geochemical evidence in support of this model is that although the degree of depletion of the highly siderophile elements in the mantle is extreme (0.5% chondritic), their relative abundances are still chondritic (O'Neill et al., 1995). More recent measurements by Becker et al. (2006) find that some highly siderophile elements in the primitive upper mantle (PUM) had ratios that are chondritic, whereas others are suprachondritic. Similar abundances have been found in lunar impact melt rocks. These authors argue that the siderophile element distributions cannot be explained simply by silicate metal equilibration. Instead they suggest that the highly siderophile element abundances reflect a late impacting event which affected both the Earth and the Moon and that on Earth a very early, highly siderophile element-enriched crust has been reworked into the modern mantle.

2.4.2.4.3 The high pressure core segregation model

Currently, the favored solution to the siderophile element problem, and the most popular model of core formation, is that silicate–metal equilibration took place at high pressures, in a deep magma ocean. Support for this model comes from very high pressure experimental studies of trace element partitioning, which show that metal–silicate partition coefficients are greatly reduced at elevated temperatures and pressures. For example Li and Agee (2001) show that at high pressures and temperatures Ni and Co become less siderophile in nature. Similarly, Chabot and Agee (2003) show that V, Cr, and Mn depletions in the mantle can be modeled in a high-temperature magma ocean. A number of recent studies suggest that the mantle has an equilibrium siderophile element signature for liquid metal–liquid silicate partitioning at 30–60 GPa and > 2,000 K, at an oxygen fugacity about 2 log units below that of the iron–wustite buffer (Chabot et al., 2005).

Experimental results of this type require the existence of a magma ocean as much as 1,000 km deep in which the metal–silicate separation took place. Most recent models of core formation (e.g. Rubie et al., 2003) require the percolation of liquid metal through a silicate magma ocean as droplets of "metal rainfall." Rubie et al. (2003) calculate a droplet diameter of about 1 cm and a settling velocity of about 0.5 $m^{-1}s$. Subsequently the metal droplets accumulate at depth into a metal layer and descend still deeper as diapirs. Precisely at which point silicate metal equilibration is established is an uncertainty in the deep magma ocean model (Fig. 2.14).

The deep magma ocean model is also successful in explaining the partitioning of light elements into the Earth's core. Gessmann et al. (2001) and Malavergne et al. (2004) have shown that at high pressures silicon solubility increases in liquid iron–alloy, although the oxygen fugacity is an important control. Wade and Wood (2005) propose a model in which the oxygen fugacity of the core increases during accretion by two log units and in which the Si content is between 5 and 7%.

2.4.2.5 The timing of core formation

Although a number of isotopic systems are potentially useful as chronometers of core formation the Hf–W isotope system is the one which is regarded as the most robust (Jacobsen, 2005). The merits of the Hf–W chronometer in establishing the time of core formation are that the isotope ^{182}Hf decays to ^{182}W with a half-life of 9 Ma, so that after

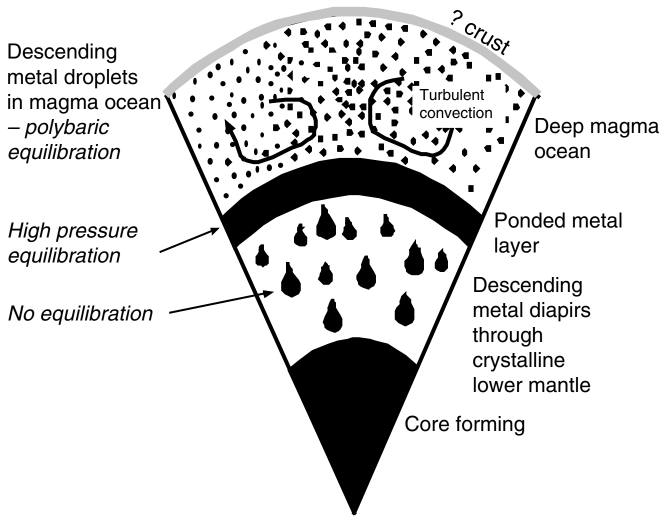

FIGURE 2.14 A generalized model for silicate–metal separation in a deep, turbulent, convecting terrestrial magma ocean. Descending metal droplets equilibrate with silicate melt and pond at the base of the magma ocean. Diapirs of metal descend to the growing core through a crystalline or partially molten lower mantle (after Rubie et al., 2003).

50 Ma the Hf–W chronometer is dead. This means that the Hf–W isotopic system is very useful in dating events that took place within the first 50 Ma of the life of the solar system. In addition the elements Hf and W display very different geochemical behavior making this isotope system particularly useful for dating core formation, for Hf is a lithophile element, with a tendency to remain in the silicate mantle whereas W is a siderophile element under highly reducing conditions, with a preference to concentrate in the Earth's metallic core (see Text Box 2.3).

Measuring W–isotope ratios is currently one of the most challenging tasks in isotope geochemistry, and over the past few years there has been great debate over whether or not the Earth has a chondritic W–isotope ratio. Recently agreement has been reached that the bulk silicate Earth (BSE) has an elevated Hf/W ratio relative to chondrites and that Earth's mantle has an excess ^{182}W relative to chondrites, indicating that the Earth's core formed during the lifetime of ^{182}Hf (Schoenberg et al., 2002). How early, is still a matter of dispute, but Yin et al. (2002) and Jacobsen (2005) provide evidence that the bulk of the metal silicate separation was complete before 30 Ma, a result which is consistent with the rapid growth of the terrestrial planets, that is, within about 10 Ma of the formation of the solar system.

A possible alternative to the above model is that the Earth's core grew gradually through the coalescing of the metal cores of planetesimals without fully equilibrating with the Earth's mantle. In this case the core formation age would be average accretion age of the two objects and would indicate a core segregation age younger than that of the time of Earth accretion (Jacobsen, 2005). These competing models can only be evaluated by further computer modeling of planetary accretion processes.

2.4.3 Was there a terrestrial magma ocean?

The central dilemma over the likely existence of a terrestrial magma ocean is that whilst there is abundant circumstantial evidence from the origin of the Earth's core and the existence of the Moon, there is no direct geochemical evidence in the Earth's mantle that such a feature ever existed.

Further lines of reasoning which have been used to infer the existence of a terrestrial magma ocean are:

- the blanketing effect of a proto-atmosphere in which it contributed to the trapping of thermal energy released from impacting (Sasaki, 1990);
- the heat generated during metal-silicate separation leading to core formation;
- the contribution from short-lived radioactive isotopes to the overall thermal budget of the new-born Earth.

TEXT BOX 2.3 Short-lived radioactive isotopes

Radioactive isotopes with short half-lives of a few million years are important in helping us to understand the history of meteorites and the earliest stages of Earth formation. The basic principles here are that if the lifetime of an isotope is short, it can only have a memory of the very earliest part of Earth history, when it was alive. Further, if there is a fractionation event affecting the parent and daughter elements during the lifetime of the isotope, this can be identified in the measured isotope ratios. There are three isotopes which are important in studies of the early Earth – ^{26}Al, ^{182}W, and ^{142}Nd and they are discussed below in order of increasing half-life.

Aluminum-26 (^{26}Al)

The radioactive isotope ^{26}Al decays to ^{26}Mg with a very short half-life of 7.2×10^5 years, and so ^{26}Al becomes extinct within a few million years of its formation. Some have likened this isotope system to the "second-hand" on the clock of the Universe. ^{26}Al was produced by explosions in supernovae early in the history of the Universe. The discovery of the excesses of the daughter isotope ^{26}Mg in very early solar system objects such as CAIs indicates that they contained ^{26}Al at the time of their formation and so must have formed within a very short time of the supernova explosion (see Section 2.3.3.2).

Tungsten-182 (^{182}W)

The Hf–W isotope system ($^{182}\text{Hf} \rightarrow {}^{182}\text{W}$) has a half-life of 9 Ma and so ^{182}Hf becomes extinct after about 50 Ma. The Hf–W chronometer, therefore, is an important tool in understanding processes which took place within the first 50 Ma of the life of the solar system.

The elements Hf and W are geochemically very different. Hf is a lithophile element, with a tendency to remain in the silicate mantle whereas W is a siderophile element with a preference for the Earth's metallic core. Hence the Hf–W isotope system is particularly useful in dating the time of core formation. It is important to ascertain whether or not there was a separation of Hf and W whilst ^{182}Hf was still live, that is, during the first 50 Ma of Earth history. Such a separation would imply that W was removed to the core, whilst Hf remained in the mantle. The logic here is that chondritic meteorites are the same material as that from which the primitive Earth was made and so should show the same Hf–isotope ratios. However, if there was a fractionation event (e.g. during core formation), whilst ^{182}Hf was alive, then the isotope ratios will be different. If such a fractionation event can be identified, then we know it must have taken place within about 50 Ma of the formation of the solar system and so provides evidence of early core formation (before 50 Ma).

Such an event can be detected from isotopic measurements of ^{182}W, measured as the ratio ^{182}W/^{183}W, compared to the ratio in primitive chondritic meteorites, and expressed in the terminology of ε-^{182}W. It is now known that Earth's mantle has an excess ^{182}W relative to chondrites, indicating that the Earth's core formed during the lifetime of ^{182}Hf (Schoenberg et al., 2002) (see Section 2.4.2.5).

Neodymium-142 (^{142}Nd)

^{142}Nd (not to be confused with the more common isotope ^{143}Nd) is the product of ^{146}Sm decay and has a half-life of 103 Ma (see Text Box 3.2, Chapter 3). ^{142}Nd therefore became extinct within the first 400–500 Ma of Earth history. Sm and Nd are both lithophile elements, and so ^{142}Nd has the potential to identify very early events in the Earth's mantle, events which took place within the first 500 Ma of Earth history. Taking chondritic meteorites as the reference point, positive or negative deviations of ^{142}Nd from the chondritic value, as expressed using the epsilon notation as ε-^{142}Nd, can be used to assess whether there was a Sm–Nd fractionation event during the first few hundred Ma of Earth history.

There are many indications that such an anomaly exists (Chapter 3, Section 3.2.3.1), the most important of which is that described by Boyet and Carlson (2005), who showed that the chondritic ϵ-^{142}Nd value is 20 ppm lower than that for terrestrial rocks, implying a ubiquitous ^{142}Nd anomaly in the Earth's mantle and a very early differentiation event in the Earth.

Whilst these thermal arguments presented here do not constitute proof of melting of the early Earth, they are persuasive. Newsom and Jones (1990) in their discussion of the evidence concluded that "there are many good reasons to believe that the early Earth was very hot. Some would go as far as to suggest that a terrestrial magma ocean was unavoidable." Similarly, Abe (1997) argued that "from a theoretical point of view it seems difficult to accrete the Earth without making some type of magma ocean."

TABLE 2.5 Magma ocean scenarios (after Abe, 1997).

Scenario	Deep or shallow magma ocean	Differentiation
1. The Earth forms in a solar nebula, blanketing effect is provided by solar gases	Deep and shallow	Shallow turbulent magma ocean with no fractionation. Differentiation takes place at lower mantle pressures and is affected by high-pressure minerals such as Mg- and Ca–perovskite
2. The Earth forms in "gas-free" space, blanketing effect of a steam atmosphere	Shallow	Upper mantle differentiation. Differentiated upper mantle material is buried in the lower mantle during the accretionary growth of the Earth
3. Giant impact	Deep and shallow	Chemical differentiation in the lower mantle is less likely due to rapid cooling, unless there is a thick transient atmosphere. The upper mantle is differentiated

2.4.3.1 Magma ocean – definitions and scenarios

The term magma ocean describes a layer, either at the surface of a planet or within its interior, which is completely or partially molten. In the case of the early Earth there are several possible scenarios. First, a distinction must be made between "transient" and "sustained" magma oceans. Transient magma oceans are those formed deep in the Earth from a single large impact which cool and solidify within a fairly short period of time. Sustained magma oceans are those surface magma oceans maintained by the thermal blanketing effect of a proto atmosphere. Second, there are "deep" and "shallow" magma oceans, and the processes of differentiation will be different in each. In a deep magma ocean differentiation will be controlled by the fractionation of high-pressure minerals such as perovskite, whereas in a shallow magma ocean it will be by olivine or garnet. Each will leave a different chemical signature in the residual melt phase. Third, it is important to identify the melt fraction in a magma ocean. "Soft" magma oceans are characterized by a high melt fraction and low viscosity, whereas a "hard" magma ocean will have a lower melt fraction and high viscosity. A soft magma ocean will experience turbulent convection such that chemical fractionation does not take place. A hard magma ocean on the other hand is more likely to become chemically fractionated, crystallizing from bottom up. Table 2.5 shows some likely magma ocean scenarios (from Abe, 1997).

2.4.3.2 Controls on magma ocean formation

The two key controls on the formation of a magma ocean are the thermal input and the melting temperature of the planetary material. The principal thermal controls are the presence of a blanketing atmosphere and the rate of delivery and size of the impactors. The blanketing atmosphere may be derived from the gases of the solar nebula, outgassed steam from the Earth or created by the impacting event itself (Table 2.5). Thus, even without impacting a thick thermal blanket can induce melting at the Earth's surface. If surface temperatures exceed 2,100 K then melting will extend deep into the Earth, into the lower mantle (Abe, 1997).

The melting temperature of the Earth's proto-mantle is governed by its initial composition. Most experimental models assume a peridotitic composition for the Earth's mantle with liquidus temperatures of about 2500 °C at 25 GPa. However, if the Earth was undifferentiated and chondritic then the melting temperature might be several hundred degrees lower (Ohtani et al., 1986; Agee, 1997). Another possibility is that the proto-mantle was originally hydrous. Again, this would significantly depress the mantle solidus (Inoue et al., 2000). A hydrous mantle could have formed through the interaction of a steam-rich atmosphere with an early crust and the mixing of that crust back into the mantle (Sasaki, 1990). Since the solubility of water increases with increasing pressure it would be possible to produce a hydrous deep mantle in which a significant quantity of water was stored (Righter et al., 1997).

2.4.3.3 Geochemical evidence for a terrestrial magma ocean

As already noted, one of the paradoxes of the terrestrial magma ocean is that whilst there are strong theoretical grounds for believing that it once existed, there is little evidence preserved in the Earth's mantle which might constitute proof of such a process. In fact, until recently, the evidence seemed to be to the contrary. The present-day mantle does not possess the physical properties of a once molten material (Takahashi & Scarfe, 1985; Ito & Takahashi, 1987), indicating that if it ever was molten, the record of such an event had been destroyed, in perhaps a turbulent early mantle (Tonks & Melosh, 1990; Solomatov, 2000).

A central test in this discussion is whether or not the magma ocean fractionated and the record of such a process is preserved in the Earth's mantle. The standard accretion model for the Earth implies a chondritic composition for the BSE (see Section 2.4.4.1, below). However, when plotted on a Mg/Si versus Al/Si ratio diagram the Earth is less siliceous than chondrite (Fig. 2.16). This problem can be resolved if the mantle was originally chondritic, but then fractionated in a magma ocean into a silica-poor, olivine-rich, peridotitic upper mantle and a silica-rich perovskite-rich lower mantle (Agee & Walker, 1988). Figure 2.15 shows the compositions of the upper mantle phase majorite and the lower mantle phase Mg–perovskite relative to a chondritic bulk Earth composition and a peridotitic upper mantle in Mg/Si–Al/Si space. It is clear from this plot that it is not possible to produce the field of mantle peridotite compositions by majorite fractionation from a chondritic melt. On the other hand it is possible to produce a "parental" peridotite by fractionating 10–20 wt% perovskite from a chondrite starting composition, as proposed by Ito and Takahashi (1987) and Agee and Walker (1988).

However, it is only recently that there has been convincing trace element and isotopic geochemical evidence to support the notion of a magma ocean. The recent ^{142}Nd isotopic study of Boyet and Carlson (2005) has shown convincingly that the Earth experienced a major differentiation event within 30 Ma of

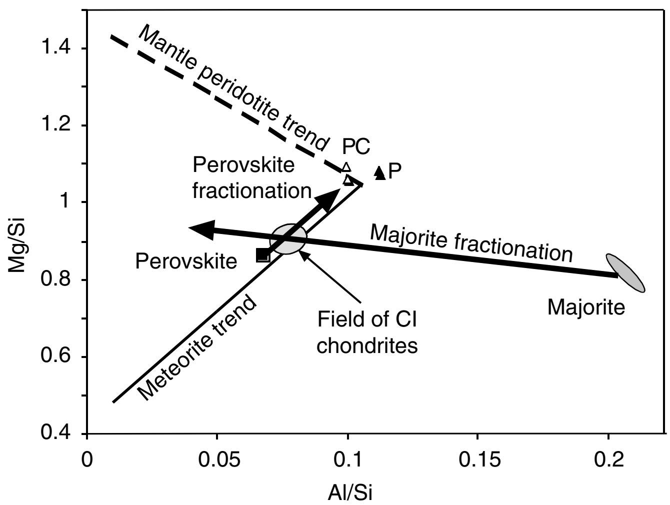

FIGURE 2.15 Mg/Si versus Al/Si (wt%) plot for CI chondrites, majorite, and perovskite. The black arrows show fractionation trends for majorite and perovskite and demonstrate that mantle peridotites cannot be produced from a chondritic starting composition by majorite fractionation but can be by perovskite fractionation. (PC – peridotite-chondrite, P – pyrolite model silicate Earth compositions). Perovskite and majorite data from Ohtani et al. (1986), Ito and Takahashi (1987), and Inoue et al. (2000).

the formation of the solar system (see Chapter 3, Section 3.2.3.1). In addition, high-pressure trace element studies have been found to support the perovskite fractionation hypothesis (Caro et al., 2005; Corgne et al., 2005). Similarly, Walter and Tronnes (2004) reported a number of nonchondritic elemental ratios in the PUM, which might be the consequence of mantle differentiation. These studies show that the fractionation of a mixture of Mg–perovskite, Ca–perovskite, and ferropericlase can explain most of the nonchondritic nature of the upper mantle, and provide important geochemical "clues" to the former existence of a terrestrial magma ocean.

2.4.4 A chondritic model for the silicate Earth

The most primitive of the chondritic meteorites are thought to represent the "raw material" from which the Earth and other terrestrial planets were accreted. These most primitive chondrites, the CI – carbonaceous chondrites (see Section 2.3.3.1), are identified by their high volatile content (they may contain up to 30 wt% of H_2O, S, and C). They lack evidence of thermal processing after their accretion and so can be treated as the least altered condensates of the solar nebula. This view is supported by a plot of element concentrations in CI chondrites against concentrations in the solar photosphere. There is a strong 1 : 1 correlation for all elements except the gaseous elements (H, He, N, O, and the inert gases) and carbon which are depleted in the chondrite.

However, when estimates of the composition of the silicate Earth are compared with primitive chondrite compositions there are a number of important differences. These may be explained in two ways. One possibility is that the primitive Earth was constructed of a chondrite other than CI chondrite, an "Earth chondrite," as is argued by Drake and Righter (2002). In this model there is no single class of meteorites that equates to an Earth composition. Alternatively, the processing of nebular material during planetary formation gave rise to fractionations which are now apparent in the Earth. In this latter model the differences between primitive chondrites and the Earth's mantle may be attributed to fractionation processes that took place within the solar nebula during chondrite formation, fractionations that took place during the accretion process and planetary formation, and fractionations that took place during early Earth differentiation, during the magma ocean stage, and core formation. Each of these possible processes is discussed below.

2.4.4.1 Solar nebula fractionations

A candidate for fractionation during solar nebula differentiation is the element silicon. Hart and Zindler (1986) showed that on a Mg/Si versus Al/Si plot mantle peridotites and chondritic meteorites plot on two quite

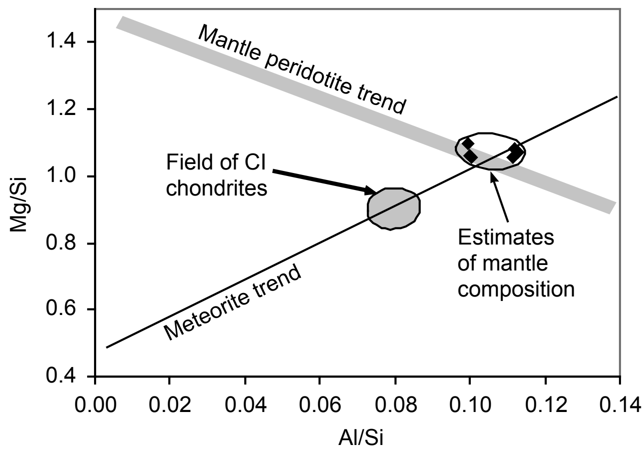

FIGURE 2.16 Mg/Si versus Al/Si plot for meteorites and mantle peridotite samples. The elliptical shaded area is the field for CI chondrites. The diamonds are estimates of mantle composition (see Chapter 3, Table 3.1), located, as expected, at the intersection between the mantle trend and the meteorite trend.

different trends (Fig. 2.16). These trends intersect at a point with a lower Mg/Si and higher Al/Si ratio than most mantle peridotites, but with higher Mg/Si and Al/Si than CI meteorites, suggesting that the Earth is Si-deficient relative to CI chondrites. The implication of this observation is that different chondritic bodies had slightly different compositions, probably related to the preferential accretion or loss of forsterite (high Mg/Si) in the solar nebula and that the Earth formed from a Si-deficient "chondritic" parent.

An alternative view, and one that has some experimental support, is that Si was partitioned into the Earth's core during core formation (Gessmann et al., 2001). If the Earth's metal core contains 7% Si then the bulk Earth and carbonaceous chondrites have the same Mg/Si ratios (Palme & O'Neill, 2003).

Further support for solar nebular fractionation comes from the compilation of Brown and Mussett (1993) who showed that the terrestrial planets have densities, which when corrected for their different internal pressure, vary significantly from that of chondritic meteorites. In fact Mars with an uncompressed density of ca. 3.7 $Mg.m^{-3}$ is the only planet which lies in the chondritic range of 3.4–3.9 $Mg.m^{-3}$. Earth, Venus, and Mercury are denser than chondrites and the Earth's Moon is less dense. These compositional differences are thought to reflect differences in the Fe/Si ratio between the different planets, which in turn reflects the fractionation of Fe from Si in relation to proximity to the Sun, during the condensation of the solar nebula, further supporting the view that the silica-depletion relative to chondrite took place in the solar nebula.

2.4.4.2 Elements fractionated during Earth accretion

The ratios of refractory to volatile lithophile elements are very different between chondritic meteorites and the silicate Earth. These fractionations are thought to have occurred during Earth accretion.

Refractory elements are present in meteorites, the Earth, and the other rocky planets in cosmic abundances and their elemental and isotopic ratios are effectively constant. In contrast, nonrefractory elements show marked variations in absolute and relative abundances with respect to each other and with respect to the refractory elements. This is seen in the extreme volatile loss of the elements H, He, C, N, and the noble gases. In addition the alkali elements (K, Na, Rb, and Cs) are depleted in the Earth's mantle relative to chondritic meteorites (Fig. 2.11). Concentrations of K and Na are approximately 20% less than those in primitive C1 chondrites, although it is possible that there is a small amount of K in the Earth's core (Gessmann & Wood, 2002).

2.4.4.3 Elements fractionated during core formation

Siderophile element concentrations in the Earth's mantle are depleted relative to chondrites (Figs. 2.12 and 2.13), most probably as a consequence of metal–silicate equilibration during core formation. Os-isotope ratios ascribed to the PUM are also different from ratios found in primitive carbonaceous chondrites (Meisel et al., 2001), also possibly a consequence of core formation.

2.4.4.4 Summary

The extent to which particular elements and isotopic ratios might be expected to be chondritic in the Earth's mantle is governed by the chemical behavior of that element during the early stages of Earth formation, as shown in Table 2.6.

2.4.5 The accretion history of the Earth

Defining the "age" of the Earth is a difficult task, for the age of the Earth may mean a number of different things. Harper and Jacobsen (1996) have shown that the age of the Earth may be defined as either the time the solar system began (T_0) or as the time at which accretion ended (T_E). However, both approaches are problematical, for the solar system began before the Earth was formed, and yet the end of accretion is very difficult to define, since the accretion process had a long tail. They suggest that a useful compromise is to define a mean accretion age for the Earth, as the time when 64% of the planetary mass had accreted. Here the main events in the accretion

TABLE 2.6 Summary of elemental behavior in the silicate Earth relative to chondrites.

Element group	Concentration relative to chondrite	Fractionation process
Light gases – H, He, N, and C	depleted	during planetary accretion
Inert gases	depleted	during planetary accretion
Volatile lithophile elements – Mg, Si, Fe, O, Ni, Na, K, Rb, Cs, S, Cu, and Pb	depleted	during planetary accretion
Silicon	depleted	during differentiation of solar nebula
Refractory lithophile elements – Ca, Al, Ti, Sc, Sr, Ba, Zr, Mo, REE, Hf, Th, U	slightly enriched	or in the core excluded from the core and so ca. 1.6 times chondrite
Weakly siderophile – V	weakly depleted	core formation
Moderately siderophile elements – W, Co, Ni, and Mo	moderately depleted	core formation
Highly siderophile elements – Au, Re, Os, PGE	strongly depleted	core formation

history of the Earth are identified. A summary table is given as Table 2.7.

The formation of the earliest matter in the solar system.
The oldest matter of the solar system is found as refractory inclusions (CAIs) and chondrules in carbonaceous chondrite meteorites. The oldest refractory inclusions from the Allende meteorite have been dated at 4,567 Ma (Amelin et al., 2002) and formed over an interval of less than a million years. T_0 therefore is 4,567 Ma. The oldest chondrules formed at the same time, at 4,567 Ma but their period of formation lasted longer, until about 4,563 Ma (Amelin et al., 2004; Haack et al, 2004).

The timescale of accretion. Increasingly evidence suggests that the accretion of the Earth was rapid and was mostly formed after 10 Ma and fully formed after 30 Ma (Jacobsen, 2005).

The formation of the Earth's core. After a period of some controversy, the most recent (and self-consistent) Hf-isotope data suggest an "early" date for the formation of the core. Given that the core grew over a period of time, dating the time of formation of the core is the same problem as dating the time of formation of the Earth. Halliday (2004) suggests that the mean accretion age of the core is about 11 Ma and that core separation was complete by 30 Ma. It is possible that core formation is, on average, earlier than accretion.

The formation of the Moon. The oldest rocks on the Moon are dated at 4,562 ± 68 Ma. However, Hf isotope evidence suggests a formation age of about 30 Ma after the formation of the solar system by 4,537 Ma. This event is thought to mark the end of accretion.

The accretion of a late veneer. Whether or not a late veneer was added to the Earth towards the end of accretion is not clear. The principal evidence comes from the elevated siderophile element chemistry of the mantle. If there was a late veneer, it had to happen after core formation. At present the evidence from the trace element chemistry is ambiguous, because these data can also be explained by the formation of the core at high pressures and temperatures in a magma ocean, or by continuous core formation with decreasing metal input. Currently, the best evidence for a late veneer comes from Os–isotope evidence, where there is a clear mismatch between the composition of the PUM and chondrite. However, even this is uncertain, as is discussed in the next chapter (Chapter 3, Section 3.2.3.4), for

Table 2.7 A chronology for the accretion of the Earth.

Event	Time (Ma)	Time from T_0 (Ma)	References
Formation of the solar system (T_0)	4567.2 ± 0.6 (4569.5 ± 0.2)	0	Amelin et al. (2002) Baker et al. (2005)
CAI formation	4567	0	Amelin et al. (2002) Bizzarro et al. (2004) Krot et al. (2005)
Chondrule formation	4567–4563	4	Amelin et al. (2002, 2004) Bizzarro et al. (2004) Haack et al, (2004) Krot et al. (2005)
Core formation (*Earth 64% formed*)	4,556 4,537	11 30	Yin et al. (2002) Jacobsen (2005)
End of core formation			
End of main growth stage	4,557	10	Jacobsen (2005)
End of accretion	4,537	30	
Differentiation of the mantle – predates formation of Moon *(see Chapter 3, Section 3.2.3.1)*	> 4,537	< 30	Boyet and Carlson (2005)
Moon formation	4,537	30	Schoenberg et al. (2002)
?? Late Veneer			Becker et al. (2005)
Oldest terrestrial materials *(see Chapter 1, Section 1.4.3)*	4,404	163	Wilde et al. (2001)
Late Heavy Bombardment *(see Chapter 6, Section 6.3.1)*	3,800–3,900	770–670	Kring and Cohen (2002)

there are a number of different models for the evolution of Os–isotopes in the Earth's mantle over time.

A late heavy bombardment. There is now good evidence that the Moon experienced a period of intense impacting at about 3.8–3.9 Ga, significantly after the normally accepted end of Earth accretion (Kring & Cohen, 2002). By inference the Earth must have experienced this same event, although attempts to find geochemical evidence of this event in the Earth's oldest sediments at Isua have been disappointing (Frei & Rosing, 2005).

Isotopic accretion modeling. As already discussed, the Earth accreted over a period of time and so defining the "age of the Earth" is not a particularly meaningful exercise. It may, however, be even more serious than this, and may be conceptually wrong, because, by its very nature, the accretion process is an open system and thereby violates one of the fundamental assumptions of geochronology (Hofmann, 2003). The recognition of this problem, that accretion is a disequilibrium process, is giving rise to a new approach to the chronology of accretion – that of isotopic accretion modeling, whereby isotopic ratios are interpreted as part of a dynamic accretion process (Kramers & Tolstikhin, 1997; Halliday, 2004). Such an approach has to make some assumptions about the nature of the unseen accreting material, its similarity or otherwise to the already formed Earth, about the degree of mixing, and about the amount of material lost in the accretion process. Although more complex, isotopic accretion modeling will become a more appropriate approach for the dynamic accretion of the Earth.